

THESIS

THREE-DIMENSIONAL ELASTICITY MODELS FOR BUCKLING OF
ANISOTROPIC AND AUXETIC BEAMS AND PLATES

Submitted by

Eltigani Hamad

Department of Civil and Environmental Engineering

In the fulfillment of the requirements

for the degree of Master of Science

Colorado State University

Fort Collins, Colorado

Fall 2015

Master's committee:

Advisor: Paul Heyliger

Rebecca Atadero

Christian Puttlitz

Copyright by Eltigani Hamad 2015

All Rights Reserved

ABSTRACT

THREE-DIMENSIONAL ELASTICITY MODELS FOR BUCKLING OF ANISOTROPIC AND AUXETIC BEAMS AND PLATES

The three-dimensional elasticity model is developed to determine the critical buckling load for isotropic, anisotropic, and auxetic beams and plates. Different beam theories are studied and compared to the elasticity theory. The study was based on the assessment of those beam theories using different beam cross-sections and boundary conditions.

The elasticity theory for anisotropic beams obtained well results for large slenderness ratios when it compared with Euler-Bernoulli theory which is considered in this study the main area of comparison study. For small values of slenderness ratio the elasticity theory obtained significant difference than the Euler-Bernoulli theory, which means that Euler-Bernoulli is weaker when it is used for short beams than long beams. The orientation of the anisotropy behavior is also studied and has showed how the buckling load can be changed due to the orientation of the elasticity modulus.

The auxetic beams behave different than the anisotropic behavior, it gives results higher and lower than the Euler-Bernoulli theory according to the slenderness ratio and the Poisson's ratio values. A significant behavior was noticed in using beams with negative Poisson's ratio which can be useful in structure mechanics field.

TABLE OF CONTENTS

ABSTRACTS.....	ii
1 INTRODUCTION.....	1
2 LITERATURE REVIEW.....	3
3 THEORETICAL DEVELOPMENT.....	14
3.1 Three-Dimensional Elasticity.....	14
3.2 Euler-Bernoulli Beam Theory.....	17
3.3 Timoshenko Beam Theory.....	18
3.4 Finite Element Models.....	21
4 RESULTS AND DISCUSSION.....	26
4.1 Isotropic beam.....	26
4.2 The Hinged-Hinged Beam.....	27
4.3 The Cantilever Beam.....	29
4.4 Convergence Study.....	30
4.5 Anisotropic Beams.....	31
4.6 Solid rectangular cross-section Beam.....	31
4.7 Open cross-section (I-Beam).....	32
4.8 Closed cross-Section (Hollow-rectangular Beam).....	37
4.9 Auxetic Beams.....	39
4.10 Solid rectangular cross-section beam.....	39
4.11 Other Geometries.....	43
5 CONCLUSIONS.....	47

BIBLIOGRAPHY 49

CHAPTER 1

INTRODUCTION

The size of structures members change according to the demand and the location, for instance, Spacecraft enhances the opportunity to observe and study the earth and planets. With the increasing for sea transport, ships are designed to carry heavy cargo mass on its board, and the demand for lightweight structure for this purpose is of importance to achieve it. Therefore, a significant demand for alternative material have come to the surface.

Cold-formed steel or aluminum thin-walled is considered as the first generation of thin-walled structures used extensively in buildings, it can be traced back to the 1850s [1]. Since steel and aluminum are isotropic materials, it is not surprising that, up to the last couple of decades, most of the research activity dealing with the analysis and behavior of thin-walled structures did not take into consideration the effect of orthotropy. The only exception is related to members containing longitudinally and/or transversely stiffened walls [2], its behavior has been modeled using the "equivalent orthotropic plate". With the advent of usage of thin-walled structures made of composite materials, it became indispensable to account for the material orthotropy, which is due to the properties and orientation of the constituents (matrix, fibres, laminae, particles, etc.) and leads to mechanical characteristics quite different from those of isotropic materials.

The main advantages of composite material, when compared with lightweight metals is the capability to achieve similar strength values with considerably less weight, an aspect that makes them ideally suited for aeronautical and aerospace applications. Composite

materials has been started to use in the 1950s and it develops according to the demand and the discovering of new materials. In civil engineering, composite has been widely used in the last few years when their well known as structural efficiency, excellent behavior under aggressive environmental conditions, and sufficiently low fabrication costs [1]. In particular, the combination of these three features is responsible for the growing demand for thin-walled composite structural members. Composite material often exhibits local and global instability in addition to brittle collapse modes, therefore, mastering these two aspects is of importance to achieve safe and economical designs, engineers should be aware of the suitable numerical and analytical tools to be able to model and study the structural behavior and load carrying capacity of thin-walled composite members.

With the development in composite structures and the continuously demand for new materials, auxetic materials is of interesting type of material, it is well known that the material will become longer as it is stretched but also become thinner in cross-section. The behavior of the material under deformation is governed by one of the fundamental mechanical properties of material is Poisson's ratio. Poissons ratio (ν) of a material is the ratio of the lateral contractile strain to the longitudinal tensile strain for a material undergoing tension in the longitudinal direction; that is, it shows how much a material becomes thinner when it is stretched. Therefore, most of the materials have a positive ν . In case of counterintuitive behavior of auxetic material, it undergoes lateral expansion when stretched longitudinally and becomes thinner when compressed.

CHAPTER 2

LITERATURE REVIEW

Buckling and post-buckling of thin-walled structures subjected to static load have been studied by many scientists about hundred years ago. The precursors that should be mentioned in almost every paper discusses stability of thin-walled structures are a group of Bernoulli and Euler [3], Timoshenko [4] and Volmir [5]. There are numerous papers dealing with linear and nonlinear stability of thin-walled structures subjected to different kind of loads. Nowadays, the presence of software packages based on FEM, make it easier to calculate the critical load for most structures and even more to determine the post-buckling behavior. The broad development of research on stability of thin-walled structures took place in the 1970s and the 1980s [6]. The ideal papers dealing with local buckling are papers written by Davis and Hancock [7] , Graves-Smith [8] , or Mulligan and Pekoz [9] .

Analyzing the behavior of isotropic material was introduced by some authors, for example, Graves-Smith [8] , Grimaldi and Pignataro [10] , Koiter [11] Krolak [12]. Interactive between different types of buckling (local, global or deformation) are discussed by many, Koiter and Pignataro [13] presented a theoretical basis for the interaction of local and global buckling. Koiter and van der Neut [14] proposed an analysis of the interaction between global and two local buckling. Byskov and Hutchinson [15] discussed the in interactive buckling of cylindrical shells.

More reviews discussed the interaction of buckling analysis of an isotropic materials can be found, in Ali and Sridharan [16], Benito and Sridharan [17], Byskov [18], Koiter and Pignataro [19], Kolakowski [20], Manevich [21], Moellmann and Goltermann [22].

There are numerous papers dealing with nonlinear problems of stability of thin-walled structures made of orthotropic materials. The pioneer works on this subject were published about 80 years ago. Sydel [23], and Smith [24] dealt with orthotropic plate buckling. Reissner and Stavsky [25] published a study on evaluating the stress for anisotropic laminated plates with arbitrarily stacked layers. The theoretical background for buckling of anisotropic plates was published by Lekhnitskii [26], Ambartsumyan [27], Ashton and Whitney [28] or Vinson and Chou [29]. There is also many works on anisotropic plates, for instance, March [30] in his work he determined the critical buckling load subjected to a plywood with angles 0, 15, 30, 45, 60, 75, and 90 to the face grain of the plate, he presented a graph to determine the effective width of plate to estimate the critical buckling load. Fraser and Miller [31] used Ritz method to determine the critical buckling load of orthotropic plates. An experimental studies on buckling of anisotropic rectangular plates with simply supported or clamped edges introduced by Mandell [32]. Noor [33] used a three-dimensional plate theories when applied to the stability analysis of multi-layered composite plates with large numbers of layers, to assess the accuracy of the classical and shear-deformation plate theories. Post-buckling analysis of orthotropic rectangular plates of symmetric cross-section presented by Chandra and Raju [34], they used Von Karman large deflection equation to estimate the load caused shortening of edges, and compared their results to previous published works.

Prahakara and Chia [35] also studied the same problem by carried out a theoretical analysis of the post-buckling behavior of orthotropic, rectangular plates with supported edges and subjected to biaxial compression. Instability for orthotropic plates subjected to pure shear was looked by Massey [36] and Brunelle and Oyibo [37].

In the 1980s and the 1990s, finite strip and finite elements approaches have been used to solve stability problems, finite strip method developed by Cheung [38] is used to study the linearity and nonlinearity of buckled structures. Dawe and others [39] developed a finite strip method based on the use of classical plate theory and first-order shear deformation plate theory to predict the post-local-buckling behavior of laminated composite plate structures subjected to uniform end shortening. Kasagi and Sridharan [40] studied the stability and the post-buckling behavior of multi-layered composite plates subjected to shear using finite strip method. They employed a trigonometric function to describe deflection along the plate and assumed a very long plates to decrease the boundary conditions influence. Mahendran and Murray [41] presented an application of the finite strip method to the elastic buckling analysis of thin-walled structures under combined loading of in-plane loading such as longitudinal compression, transverse compression, shear and bending. Elastic nonlinear response of locally buckled thin-walled beam-columns is also studied using the finite strip method by Davids and Hancock [42], they combined the strip method with the influence coefficient method of nonlinear analysis of beam-columns. A similar work presented by Eccher [43], he presented the elastic buckling analysis of thin-walled structures by the isoparametric spline finite strip assuming linear fundamental state.

The finite element method used by Hu and Tzeng [44] to analyze the stability of rectangular plates with elastic fibrous composite laminates with different arrangement of

layers. They employed the commercial software ABAQUS to analyze simply supported or clamped plates subjected to eccentric compressive load. Bao et al. [45] used the FEM to analyze the critical stress for flat rectangular orthotropic thin plates with different boundary conditions. He also investigated the beam-columns made of anisotropic materials. Barbero and Tomblin [46] used the Southwell method to determine the critical buckling load about the strong and weak axes, they compared the experimental results with the theoretical ones receiving a good agreement with a difference percentage less than 6.2%. Gupta and Rao [47] studied the stability of a thin cantilever beam with a Z-cross-section made of two (45/-45) or three (0/45/0) layered laminates. The authors employed the finite element method to analyze the model. In the last decade, Awrejcewicz and co-authors have published monographs [48–50] devoted to dynamics and statics of plates and shells made of isotropic and orthotropic materials. They have presented a broad spectrum of analytical and numerical methods applied to solve problems of static stability and vibration of thin-walled structures. Despite the fact that since the first work on stability of the thin-walled structures, has passed more than a century, stability and critical load subjected to the thin-walled structures is still an active topic. Recently there are some papers discussing the same problem from different views, some of these publications are mentioned below.

There are some published works that should be mentioned, Szymczak and Chroscielewski from the Gdansk University of Technology, Tomski and others from the Czestochowa University of Technology, Teter from the Lublin University of Technology, Garstecki, Magnucki and Zielnica from the Poznan University of Technology, and Humer from Johannes Kepler University. Szymczak [51] studied the stability of the construction of halls modelled as thin-walled frames. It has revealed that the obtained bifurcation point is

unsymmetrical and unstable, which can lead to a reduction of critical loads due to some geometrical and loading imperfections. Chroscielewski et al. [52] discussed the effect of initial deflection on torsional buckling load of the thin-walled I-beam column. The authors have observed and analyzed the localization of the local buckling modes, he compared the numerical results obtained using the theory of thin-walled members with the non-linear 6-parameter theory of shells. Tomski [53–55] studied the stability of the slender geometrically nonlinear system supported at the loaded end by a spring of linear characteristic and subjected to non-conservative (generalized Becks) loading. Tomski [56] also dealt with problem of global instability of slender systems with imperfections subjected to Euler load, he presented the results of analytical, numerical and experimental for his model. Teter and Kolakowski [57, 58] investigated the instability behavior of thin-walled beam-columns with intermediate stiffeners, they analyzed the interaction between the local and global buckling and the influence of this interaction on buckling load. Rezeszut and Garstecki [59, 60] proposed a method to represent the initial imperfections as linear superposition of a limited number of buckling Eigen modes, in their work the studied the linear and non-linear stability analyses of double sigma members in the elastic range. They also came with a result that the interaction between the global and local buckling can result in excessive sensitivity to imperfections and in unstable behavior. Magnucki with his team [61–63] have published a few papers devoted to global and local stability of cold-formed thin-walled channel beams with open or closed flanges. They presented a simple analytical description and calculations, and the FEM analysis of selected beams. The main area of Zielnicas interest are sandwich conical and cylindrical shells. In his latest papers, Zielnica et al. presents a derivation of the stability equation and the method of solution for an elastic-plastic open conical shell made of orthotropic materials [64].

They take into consideration a bi-layered open conical shell subjected to longitudinal force and lateral pressure. The solution for a freely supported sandwich cylindrical shell with unsymmetrical faces, loaded by longitudinal forces, transversal pressure and shear, can be found in [65]. Paper [66] presents a buckling analysis and equilibrium stability paths of the sandwich conical shell with unsymmetrical faces subjected to combined load. Based on Ressiner theory for plane deformation, Humer [67] investigated the buckling and post-buckling behavior of beams subjected to axial compressibility and shear deformation. He derived the equilibrium equation for statically determinate and indeterminate combinations of boundary conditions representing the four fundamental buckling cases. The bifurcation load is determined and the influence of shear on the buckling behavior is investigated. Kolakowski et al. [68–70] have used the asymptotic Koiter theory for conservative systems to analyze the interactive buckling and the post-buckling behavior of thin-walled columns with different cross-sections. In [68], Kolakowski and Kowal-Michalska analyse an influence of the axial extension mode on the interactive buckling of thin-walled channel subjected to uniform compression. Multi-cell thin-walled columns of triangular and rectangular cross-sections have been investigated for load carrying capacity by Krolak [71–73]. He compared the theoretical and experimental investigations with FEM calculation results.

Thin-walled beam-columns with open and closed cross-sections subjected to compression or pure bending have been widely discussed as well. Loughlan et al. have conducted a numerical analysis and experimental tests on lipped cross-section [74], I-section and box-section [75] struts. He employed the FEM package software ANSYS to analyze the numerical analysis. They have examined the buckling and post-buckling behavior and the failure mode of thin-walled struts assuming the elastic-plastic material behavior. They

have proposed FEM models and procedures for determine the coupled local-distortional interactive response of thin-walled lipped channel sections [74]. Ovesy have employed the finite strip method [76] to carry out a numerical analysis and have compared the obtained results with the FEM and experiments. The post-buckling behavior, the load carrying the capacity estimation and the failure mode of stainless steel stub columns [77] and multilayered plate structures have been analyzed by Kotelko, Kowal-Michalska, Rhodes and others. Rhodes and Macdonald [78, 79] presented a summary of the recent research on stability, post-buckling behavior and load carrying capacity of cold-formed steel members and structures, in [78] they studied the behavior of thin-walled members under various loading. Rhodes and his students in [79] have studied the effects of end fixity on plain channel column behavior, the effects of transverse impact on struts and the damaged strut capacity and the large deflection behavior of slender rings under diametrically opposed point loads.

The significant development in computational methods has allowed to determine the buckling and post-buckling analysis of thin-walled structures. In recent years, two competitive software codes allowing to determination of critical load for uncoupled and coupled buckling have been developed. They enable also analyzing the post-buckling behavior of thin-walled beam-columns. GBT [80] one of these methods, is based on the generalized beam theory. The second one is called CFSM, has been developed by Shafer [81] and is based on the constrained finite strip method.

Auxetic materials has opened the door towards inventing new type of materials that could have negative Poissons ratio. This unusual property was rst reported in 1944 when iron pyrites single crystals were described as having a negative Poissons ratio, a phenomenon, which was regarded as an anomaly and attributed to twinning defects [82], since then

and most particularly in the last two decades, auxetic behavior was introduced in various materials ranging from molecular level systems [83–87], metals [88], silicates [89] and zeolites [90] to micro-structured materials such as foams (35-39), and micro-structured polymers [91, 92].

Lakes was the first one who manufactured auxetic foams, in [93], he studied the behavior of the stress concentration factor when the material components exhibit a negative Poisson's ratio, he found that the stress concentration factors are reduced in some situations and unchanged or increase in others. Lakes [94], discussed the negative Poisson's ratio for anisotropic materials, he has claimed that the value of Poisson ratio bounds between $(-\infty < \nu < \infty)$ than in isotropic materials that bounds between $(-1 < \nu < 0.5)$, and he discussed how the stack of the cells can affect the behavior of the material. In [95], Lakes introduced the auxetic material and its behavior when it subjected to external loads, for instance, honeycombs with inverted cells, anisotropic materials including a few natural single crystals, some synthetic off axis composite laminates have all reported to have a negative Poisson's ratio when subjected to axially loads in some direction. He also presented the useful aspects of having negative Poisson's ratio for some materials. Evans and Alderson [91] presented some examples of auxetic materials, and the effect of negative Poisson's ratio on their mechanical properties and how these new materials can be used in applications.

H. Obrecht [96] studied the properties of auxetic materials, such as, Shear modulus which depends inversely on $1+\nu$ and thus tends to infinity as ν approaches its negative limit of -1, therefore, such a dramatic increase must also effect the load carrying behavior. He has found out that the bifurcation stresses increase dramatically as ν approaches -1. He has also concluded that the angle of the cell wall plays the major role in estimating the bifurcation

stress values. Pozniak et al. [97] studied the deformation of a two-dimensional isotropic material forming a square sample with two sides fixed and the other two remaining under uniform compression load. It revealed that for negative Poissons ratio, at the corner of the sample model, it behaves in a counterintuitive way, the material in those domains moves in the direction opposite to the pressure applied which considered as a locally negative compliance.

Grima et al. [98] presented a new explanation for achieving auxetic behavior in foam cellular materials, they called it's "rotation of rigid units" mechanism, the cellular structure is volumetrically compressed and then frozen in the compressed conformation, this deformation results in auxeticity behavior. Wadee et al. [99] investigated the behavior of tubes subjected to pure bending using Timoshenko theory, the tubes material is constructed either of orthotropic materials or of different Poissons ratio. The revealed results show that for certain values of ν the interaction between buckling modes reduces the moment significantly. Moreover it is found that post-buckling behavior is more severe and may lead to kinking failure if the material is stressed beyond its elastic limit. Karnesis and Burriesci [100] also studied the mechanical properties of auxetic tubes based on hexagonal honeycombs. They showed that using of auxetic structures can result in significantly improved buckling behavior compared to similar non-auxetic arrangements. They solved the problem with matching the analytical with numerical approaches.

Buckling and vibration of isotropic circular auxetic plates under various boundary conditions discussed by Lim [101], he showed that as the Poisson's ratio negativity increases, the critical buckling load gradually reduced. In the case of vibration the decrease in Poisson's ratio not only decreases the fundamental frequency, but the decrease becomes very rapid as the Poisson's ratio approaches its lower limit. Auxetic behavior into thin

walled discussed by Weller [102], in his study he examined the feasibility of inducing auxetic behavior into thin-walled structures, and the shear stiffness enhancement. For a membrane plate, he revealed the following results, it is possible to induce an auxetic behavior in thin-walled structures by out-of-plane corrugations, and using the geometric parameters it is possible to change, and in some cases to optimize to some extent, the resulting effective elastic properties. Shufrin et al. [103] presented a study for materials composed of hollow spheres. It is shown that the negative Poisson's ratio in this material is due to the high ratio between tangential (shear) to normal stiffness of a thin-wall hollow sphere. It has been shown that the structural parameters of the assemblies, such as the wall thickness to sphere radius ratio and the contact area between the spheres control the mechanical properties of the hollow sphere materials.

It has also been found that a decrease in the contact area between the spheres, which corresponds to weak connection significantly enhance the auxetic property, while not affecting the relation between the shear and Young's modulus.

Brighebt [104] in his paper has used the phrase smart structures as the significant features of auxetic behavior, he studied the response of layered plates, and presented the mechanical characteristic. He showed that the plates bending stiffness can be accurately designed by simply varying the Poisson's coefficient of only one thin ply of the layered plate, without changing its thickness and mechanical properties. He also proposed the values to measure the geometrically nonlinear stiffening effect behavior in presence of auxetic layer.

Abdul-Aziz, Limbert, Young, and Beresford-west [105] have used ABAQUS to present the behavior of auxetic materials, they introduced a new approaches in generating the mesh for their models, the approach was to generate mesh directly from 3D images which is considered to provide fast and accurate values to explore the structure properties.

CHAPTER 3

THEORETICAL DEVELOPMENT

Convergence study is conducted to determine the critical buckling load for isotropic and anisotropic materials using ABAQUS software. Humer [67] studied the behavior of thin-walled beam under shear deformable using two-dimensional elasticity theory, in his paper he investigated the influence of shear on the buckling behavior for different beam configuration. Heyliger [106] proceed through the work of Humer to study the three-dimensional elasticity theory, he used Ritz model approximation to introduce the generalized eigenvalue matrix. Mohammad and Archibald [107] studied the elastic local instability of anisotropic composite beams buckling under nonlinear varying, uni-axial compressive forces. they used Galerkin method to introduce the plate equilibrium equations.

3.1 Three-Dimensional Elasticity

In order to study the elastic behavior of a body subjected to different kind of loads, we shall determine the entire stress and strain components of it and understand the stress-strain relation. There are nine components define the stress tensor at any given point on the body having the Cartesian system (x,y,z) Figure1, components of stress acting on an area normal to the x-axis $\sigma_x, \tau_{xy}, \tau_{xz}$, components of stress acting on an area normal to the y-axis $\sigma_y, \tau_{xy}, \tau_{yz}$ and components acting on an area normal to the z-axis $\sigma_z, \tau_{zz}, \tau_{yz}$.

If we know the stresses in three mutually perpendicular areas, we can determine the stress acting on any area passing through the same point.

$$T_x^n = \sigma_x e_x + \tau_{xy} e_y + \tau_{xz} e_z \quad (3.1)$$

$$T_y^n = \tau_{yx} e_x + \sigma_y e_y + \tau_{yz} e_z$$

$$T_z^n = \tau_{zx} e_x + \tau_{zy} e_y + \sigma_z e_z$$

where T_x^n, T_y^n, T_z^n are components of stress which act on an area with the arbitrary normal direction.

To present the anisotropic material Hooke's law is assumed that such materials are homogeneous in which the directional properties at a specific point in the material represent the directional properties of the whole element. Stress and strain relation are applied to an anisotropic body will result in linearly components of strain. There are nine stress terms σ_{ij} where i,j refer to the global coordinate system x,y,z. Referring to the x,y,z directions in terms of integers 1,2,3, the generalized Hooke's law may be written as:

$$\sigma_{ij} = C_{ijkl} \epsilon_{kl} \quad (3.2)$$

where C_{ijkl} form are termed the material stiffness, and ϵ_{kl} is the mathematical strain tensor. Similarly the stress-strain tensor is given by:

$$\epsilon_{ij} = S_{ijkl} \sigma_{kl} \quad (3.3)$$

where the S_{ijkl} are referred to as the material compliances. the tensors C_{ijkl} and S_{ijkl} contains 81 terms, and from the definition of the components of the stress and strain tensors, the number of independent terms reduces to 36:

$$C_{ijkl} = C_{ijlk}, C_{ijkl} = C_{jikl}$$

For isotropic material, symmetry is introduced and the system can be reduced significantly. When strains are infinitesimal, the Cauchy strain components are linked with the three displacement components u,v and w in the x,y and z direction as

$$\begin{aligned} \epsilon_1 = \epsilon_{11} &= \frac{\partial u}{\partial x} & \epsilon_2 = \epsilon_{22} &= \frac{\partial v}{\partial y} & \epsilon_3 = \epsilon_{33} &= \frac{\partial w}{\partial z} \\ \epsilon_4 = \gamma_{23} &= \frac{\partial v}{\partial z} + \frac{\partial w}{\partial y} & \epsilon_5 = \gamma_{13} &= \frac{\partial u}{\partial z} + \frac{\partial w}{\partial x} & \epsilon_6 = \gamma_{12} &= \frac{\partial u}{\partial y} + \frac{\partial v}{\partial x} \end{aligned} \quad (3.4)$$

The general constitutive relation can be shown in matrix form as follow

$$\begin{pmatrix} \sigma_1 \\ \sigma_2 \\ \sigma_3 \\ \sigma_4 \\ \sigma_5 \\ \sigma_6 \end{pmatrix} = \begin{vmatrix} C_{11} & C_{12} & C_{13} & 0 & 0 & 0 \\ C_{21} & C_{22} & C_{23} & 0 & 0 & 0 \\ C_{13} & C_{23} & C_{33} & 0 & 0 & 0 \\ 0 & 0 & 0 & C_{44} & 0 & 0 \\ 0 & 0 & 0 & 0 & C_{55} & 0 \\ 0 & 0 & 0 & 0 & 0 & C_{66} \end{vmatrix} \begin{pmatrix} \epsilon_1 \\ \epsilon_2 \\ \epsilon_3 \\ \epsilon_4 \\ \epsilon_5 \\ \epsilon_6 \end{pmatrix} \quad (3.5)$$

This relation will be used later in this study to determine the critical buckling load for orthotropic materials.

3.2 Euler-Bernoulli Beam Theory

The Euler-Bernoulli is considered the simplest theory to to determine the deformation of beams. It only considers the transverse displacement of the beam, beside neglecting the Poisson's ratio effect assumes that the cross-section remains perpendicular to the neutral axis and allows for the reduction to one dimension. The displacement field of the Euler-Bernoulli beam is given by

$$u(x, y, z) = -z \frac{\partial w}{\partial x} \quad (3.6)$$

$$v(x, y, z) = 0 \quad (3.7)$$

$$w(x, y, z) = wx \quad (3.8)$$

where u, v , and w represents the displacement in the x,y, and z directions, respectively. The transverse displacement is represented by the variable w . Now consider a straight elastic beam with linearly elastic end constraints. Let K_1, K_2 refer to the elastic constants for the rotational springs, and k_1, k_2 refer to the elastic constants for the extensional springs. let an axial compressive load P be applied to the both ends supports.

The column remain straight until the value of the compressive load increase to a critical value at which any small lateral disturbance will cause the column to buckle.

For a Beam subjected to axial load and under specific boundary conditions, the equation given by Euler [4] to determine the minimum load that initiates a buckled state which is referred to as the critical buckling load or Euler buckling load is given by

$$P_E = \frac{\pi^2 EI}{L_e^2} \quad (3.9)$$

where L_e is the effective length which is depend on the applied boundary conditions. In Euler equation derivation, it assumes that the only non-zero are the axial strain along the beam length. This formula is considered significantly accurate for beams with sufficiently large slenderness ratio, which means the length of beam is relatively large compared with its cross-section.

3.3 Timoshenko Beam Theory

For relatively short beams, adjustment can be made to predict the critical buckling load. Humer [67] has recently given an adjustment formula where shear deformation is incorporated into the displacement field. He used the constitutive equations to link the resultant stress to the generalized strain measures, extensional stiffness, shear stiffness, and bending stiffness are adopted as proportionally coefficients.

$$N = D\epsilon \quad (3.10)$$

$$Q = SY \quad (3.11)$$

$$M = BK \quad (3.12)$$

The proportionality coefficient D, S and B are referred to as extentional stiffness, shear stiffness, and bending stiffness. In cases that the shear stiffness is greater than the extensional stiffness, i.e., $\eta > 1$ the material is considered as auxetic material. On the other hand, when the extensional stiffness exceeds the shear stiffness, this case represent most of the conventional materials. Later these concepts will be discussed in more details. Humer provides a one-dimensional formula that include the elastic longitudinal modulus E , the shear modulus G , the cross-sectional area A , and the second moment of the area

about the bending axis I . He also used the shear-correction factor k_s , which depends on Poisson's ratio ν . For different types of boundary conditions, Humer provided a number of exact results. for instance, for simply supported beam he provides the following equation

$$\frac{P_{cr}}{P_e} = \frac{1}{2} \frac{\eta}{\eta - 1} \frac{\lambda^2}{\pi^2} \pm \sqrt{\left(\frac{\eta}{\eta - 1}\right)^2 \frac{\lambda^4}{4\pi^4} - n^2 \frac{\eta}{\eta - 1} \frac{\lambda^2}{\pi^2}} \quad n = 1, 2, 3, \dots \quad (3.13)$$

For clamped-clamped beam

$$\frac{P_{cr}}{P_e} = \frac{1}{2} \frac{\eta}{\eta - 1} \frac{\lambda^2}{\pi^2} \pm \sqrt{\left(\frac{\eta}{\eta - 1}\right)^2 \frac{\lambda^4}{4\pi^4} - 4n^2 \frac{\eta}{\eta - 1} \frac{\lambda^2}{\pi^2}} \quad n = 1, 2, 3, \dots \quad (3.14)$$

where λ is the slenderness ratio and is given by

$$\lambda = L \sqrt{\frac{A}{I}}$$

The relationship between the bending stiffness and the shear stiffness μ is given by

$$\eta = \frac{K_s G}{E}$$

and finally n refers to the mode number associated with the buckling load, which is typically associated with the sine shape function given by

$$v(x) = A \sin \frac{n\pi z}{L} \quad (3.15)$$

Here $v(x)$ is the transverse displacement of the beam centroid along the length of the beam in the z direction. For both support conditions, the behavior of Timoshenko beam model prediction is shifted as the parameter η tends to unity. Humer in his work [67] he

explained that in more details and it is noted that when $\eta = 1$ the critical load changes in behavior for auxetic materials. In this work, we consider a three-dimensional solid whose cross-section coordinates are defined in the (x, y) direction and with length in the z direction. As mentioned before, the solid material is assumed to be orthotropic. An approximately solutions according to the energy method, for a beam under an axial force P the total potential energy can be written as

$$\Pi = U - W \quad (3.16)$$

where U is the strain energy and W is the potential energy of the body force vector f , the surface traction vector T excluding the axial force, and the applied axial force P , with

$$U = \int_V \frac{1}{2} \sigma_{ij} \epsilon_{ij} dV \quad W = \int_A \frac{P}{A} \Delta L dx dy + \int_V f_i u_i dV + \int_S t_i u_i dS \quad (3.17)$$

Here u_i are the components of displacement, A is the cross-sectional area of the solid perpendicular to P , and ΔL is the distance over which the axial force P moves. i, j represent the indicial notation for the Cartesian coordinates ($x_1 = x, x_2 = y, \text{ and } x_3 = z$) where the z -direction is the long direction of the solid.

The axial force P is assumed to act through a uniform compressive normal traction P/A over the entire face of the beam cross-section, which means that the axial force $(P/A)dxdy$ moves an amount that varies with the cross-section coordinates (x,y) . The distance for a specific location within the cross-section (x,y) can be written as

$$\begin{aligned}\Delta L &= \int_0^L (ds - dz) = \int_0^L \{[(dz)^2 + (du)^2 + (dv)^2]^{1/2} - dz\} = \\ &= \int_0^L \{[1 + (\frac{du}{dz})^2 + (\frac{dv}{dz})^2]^{1/2} - 1\} dz \simeq \frac{1}{2} \int_0^L [(\frac{du}{dz})^2 + (\frac{dv}{dz})^2] dz\end{aligned}\quad (3.18)$$

Three-Dimensional Elasticity Equation

The governing equations used for this study are the three-dimensional equations of linear elasticity with an orthotropic constitutive tensor. For solid beam with axial compressive applied load only, and with neglecting the body forces, the formula is expressed by

$$0 = \int_V [\sigma_{ij} \delta \epsilon_{ij} - P \frac{\partial v}{\partial x} \frac{\delta \partial v}{\partial x} - P \frac{\partial u}{\partial x} \frac{\delta \partial u}{\partial x}] dV \quad (3.19)$$

Here P is the compressive buckling load, V is the volume of the beam, and δ is the variational operator.

3.4 Finite Element Models

The solution to the three-dimensional elasticity solutions utilizes Ritz-based approximations. The general form for the three displacements and their variations as required by

virtual work can be expressed as

$$\begin{aligned}
u(x, y, z) &= \sum_{p=1}^n c_p \Psi_p^u(x, y, z) & \delta u(x, y, z) &= \psi_i^u(x, y, z) \\
v(x, y, z) &= \sum_{p=1}^n d_p \Psi_p^v(x, y, z) & \delta v(x, y, z) &= \psi_i^v(x, y, z) \\
w(x, y, z) &= \sum_{p=1}^n e_p \Psi_p^w(x, y, z) & \delta w(x, y, z) &= \psi_i^w(x, y, z)
\end{aligned} \tag{3.20}$$

where c_p, d_p, e_p are unknown constants and ψ_p is the approximation function for each respective direction. For accurate solutions large number of these approximation terms for each displacement component. polynomial series are used for the cross-section and the axial length of the beam then they combined together. General formula was introduced by Visscher and co-workers [108], which is given as

$$\psi_p^u(x, y, z) = x^i y^j z^k \tag{3.21}$$

By substitution the general Ritz approximations into virtual work, it leads to the generalized eigenvalue problem that can be represented in matrix form as

$$\begin{bmatrix} [K^{11}] & [K^{12}] & [K^{13}] \\ [K^{21}] & [K^{22}] & [K^{23}] \\ [K^{31}] & [K^{23}] & [K^{33}] \end{bmatrix} \begin{Bmatrix} \{c\} \\ \{d\} \\ \{e\} \end{Bmatrix} = P \begin{bmatrix} [B^{11}] & [0] & [0] \\ [0] & [B^{22}] & [0] \\ [0] & [0] & [0] \end{bmatrix} \begin{Bmatrix} \{c\} \\ \{d\} \\ \{e\} \end{Bmatrix} \tag{3.22}$$

with

$$[K^{11}]_{ij} = \int_V [C_{11} \frac{\partial \psi_i^u}{\partial x} \frac{\partial \psi_j^u}{\partial x} + C_{55} \frac{\partial \psi_i^u}{\partial z} \frac{\partial \psi_j^u}{\partial z} + C_{66} \frac{\partial \psi_i^u}{\partial y} \frac{\partial \psi_j^u}{\partial y}] dV \tag{3.23}$$

$$[K^{11}]_{ij} = \int_V [C_{12} \frac{\partial \psi_i^u}{\partial x} \frac{\partial \psi_j^v}{\partial y} + C_{66} \frac{\partial \psi_i^u}{\partial y} \frac{\partial \psi_j^v}{\partial x}] dV \quad (3.24)$$

$$[K^{13}]_{ij} = \int_V [C_{13} \frac{\partial \psi_i^u}{\partial x} \frac{\partial \psi_j^w}{\partial z} + C_{55} \frac{\partial \psi_i^u}{\partial z} \frac{\partial \psi_j^w}{\partial x}] dV \quad (3.25)$$

$$[K^{22}]_{ij} = \int_V [C_{22} \frac{\partial \psi_i^v}{\partial y} \frac{\partial \psi_j^v}{\partial y} + C_{44} \frac{\partial \psi_i^v}{\partial z} \frac{\partial \psi_j^v}{\partial z} + C_{66} \frac{\partial \psi_i^v}{\partial x} \frac{\partial \psi_j^v}{\partial x}] dV \quad (3.26)$$

$$[K^{23}]_{ij} = \int_V [C_{23} \frac{\partial \psi_i^v}{\partial y} \frac{\partial \psi_j^w}{\partial z} + C_{44} \frac{\partial \psi_i^v}{\partial z} \frac{\partial \psi_j^w}{\partial y}] dV \quad (3.27)$$

$$[K^{33}]_{ij} = \int_V [C_{33} \frac{\partial \psi_i^w}{\partial z} \frac{\partial \psi_j^w}{\partial z} + C_{44} \frac{\partial \psi_i^w}{\partial y} \frac{\partial \psi_j^w}{\partial y} + C_{55} \frac{\partial \psi_i^w}{\partial x} \frac{\partial \psi_j^w}{\partial x}] dV \quad (3.28)$$

$$[B_{ij}^{11}] = \int_V \frac{\partial \phi_i^u}{\partial x} \frac{\partial \phi_j^u}{\partial x} dV \quad (3.29)$$

$$[B_{ij}^{22}] = \int_V \frac{\partial \phi_i^v}{\partial y} \frac{\partial \phi_j^v}{\partial y} dV \quad (3.30)$$

This study has conducted to determine the validity and the accuracy for some of the buckling theories, ABAQUS software based on finite element theory which is used the elastic constitutive law for the stress-strain relation. the linear elasticity in an orthotropic material can be defined by giving the nine independent elastic stiffness parameters as

follows

$$\begin{pmatrix} \sigma_{11} \\ \sigma_{22} \\ \sigma_{33} \\ \sigma_{12} \\ \sigma_{13} \\ \sigma_{23} \end{pmatrix} = \begin{pmatrix} C_{1111} & C_{1122} & C_{1133} & 0 & 0 & 0 \\ & C_{2222} & C_{2233} & 0 & 0 & 0 \\ & & C_{3333} & 0 & 0 & 0 \\ & & & C_{1212} & 0 & 0 \\ & \text{sym} & & & C_{1313} & 0 \\ & & & & & C_{2323} \end{pmatrix} \begin{pmatrix} \epsilon_{11} \\ \epsilon_{22} \\ \epsilon_{33} \\ \gamma_{12} \\ \gamma_{13} \\ \gamma_{23} \end{pmatrix} = [D^{el}] \begin{pmatrix} \epsilon_{11} \\ \epsilon_{22} \\ \epsilon_{33} \\ \gamma_{12} \\ \gamma_{13} \\ \gamma_{23} \end{pmatrix}$$

The engineering constants defined as follows

$$C_{1111} = E_1(1 - \nu_{23}\nu_{32})\Upsilon$$

$$C_{2222} = E_2(1 - \nu_{13}\nu_{31})\Upsilon$$

$$C_{3333} = E_3(1 - \nu_{12}\nu_{21})\Upsilon$$

$$C_{1122} = E_1(\nu_{21} + \nu_{31}\nu_{23})\Upsilon = E_2(\nu_{12} + \nu_{32}\nu_{13})\Upsilon$$

$$C_{1133} = E_1(\nu_{31} + \nu_{21}\nu_{32})\Upsilon = E_3(\nu_{13} + \nu_{12}\nu_{23})\Upsilon$$

$$C_{2233} = E_2(\nu_{32} + \nu_{12}\nu_{31})\Upsilon = E_3(\nu_{23} + \nu_{21}\nu_{13})\Upsilon$$

$$C_{1212} = G_{12}$$

$$C_{1313} = G_{13}$$

$$C_{2323} = G_{23}$$

$$\text{where } \Upsilon = \frac{1}{1 - \nu_{12}\nu_{21} - \nu_{23}\nu_{32} - \nu_{31}\nu_{13} - 2\nu_{21}\nu_{32}\nu_{13}}$$

ABAQUS manual provides restrictions on the elastic constants due to the material stability as follows

$$C_{1111}, C_{2222}, C_{3333}, C_{1212}, C_{1313}, C_{2323} > 0$$

$$|C_{1122}| < (C_{1111}C_{2222})^{1/2}$$

$$|C_{1133}| < (C_{1111}C_{3333})^{1/2}$$

$$|C_{1133}| < (C_{1111}C_{3333})^{1/2}$$

$$|C_{2233}| < (C_{2222}C_{3333})^{1/2}$$

$$\det(C)^{el} > 0$$

CHAPTER 4

RESULTS AND DISCUSSION

4.1 Isotropic beam

The study of the behavior of anisotropic material for thin-walled beam is the main target of this study, however, initially it is important to validate the used method by applying it on solid isotropic material. Rectangular beam has been chosen for this convergence study. The beam has 1 m x 1 m cross-section and the length varied from 10 m to 50 m, since it is important to consider shorter beams as well as long beams. Euler Formula equ. 3.9 in which the beam is considered as a slender beam and perfectly elastic, the beam remain straight until the compressive force reach the critical load. Humer [67] derived two beam configuration equations, the hinged-hinged beam and the cantilever beam equation 3.13, 3.14 as a ratio between the critical load taking into account both the influence of axial compressibility and shear deformation and the Euler buckling load.

In this study ABAQUS software is adopted as a convergence study for Humer equations and other beam theories that will discussed later.

The boundary conditions used for various configuration are varied according to the adopted theory. In the classical and Timoshenko beam theories, hinged supports are associated with zero transverse displacement and zero resultant end moments. For elasticity theory, the transverse displacement is zero as well and the axial traction components T_z at the end are zero. For the cantilever beam, the classical beam theory specifies that the transverse displacement and its first derivative are both zero. In the Timoshenko theory, the displacement and the section rotation are specified to be zero. In elasticity

theory, all three of the displacement components are specified to be zero but none of their derivatives. For the free end, the beam theories enforce zero resultant shear and moment. For the elasticity model, the free end is traction free and hence all components of the stress traction T_x, T_y, T_z vector are equal to zero as shown in Table 4.1 and 4.2, where w is the transverse displacement, V_x, M_{xx} the resultant shear and moment, respectively .

TABLE 4.1: Boundary condition configuration for simply-supported beam

Theory	Pinned-end		Pinned-end	
	Transverse Displacement	Resultant shear/Mo-ment	Transverse Displacement	Resultant shear/Mo-ment
Classical	$w=0$	$M_{xx} = 0$	$w=0$	$M_{xx} = 0$
Timoshenko	$w=0$	$M_{xx} = 0$	$w=0$	$M_{xx} = 0$
Elasticity	$w=0$	$T_z = 0$	$w=0$	$T_z = 0$

TABLE 4.2: Boundary condition configuration for cantilever beam

Theory	Fixed-end		Free-end	
	Displacement/ Rotation	Resultant shear/Mo-ment	Displacement/ Rotation	Resultant shear/Mo-ment
Classical	$w=0, \frac{\partial w}{\partial x} = 0$	—	—	$V_x, M_{xx} = 0$
Timoshenko	$0, \frac{\partial \phi}{\partial x} = 0$	—	—	$V_x, M_{xx} = 0$
Elasticity	$u, v, z = 0$	—	—	$T_x, T_y, T_z = 0$

4.2 The Hinged-Hinged Beam

Timoshenko and Gere [4] refer to the case of simply supported beam as the fundamental case of buckling. As mentioned before, in Timoshenko theory the boundary conditions at the end supports associated with zero bending moment, therefore, the derivative of the angle rotation is zero at the supports.

$$\left[\frac{\partial \phi}{\partial x}\right]_{x=0} = 0 \quad \left[\frac{\partial \phi}{\partial x}\right]_{x=L} = 0$$

By applying the boundary conditions, Humer [67] derived equation 3.13 to represent the critical buckling load for simply supported beams, it is assumed that the shear stiffness is smaller than the extensional stiffness, $\eta < 0.5$, which represents the most common situation for conventional types of structures or in other meaning, those materials that have a positive Poisson's ratio. For these values of η , the expression under the root always remains greater than zero regardless of the choice of n . The results for different values of Poisson's ratio shown in Table 4.3. As shown in Figure 4.1 it is obvious that the generalized elastica buckles at lower intensities of the compressive force if the stiffness ratio is $\eta < 1$. The critical loads of the first three buckling modes are plotted against the slenderness for a poisson ratio of $\nu = 0.5$. the dotted lines represent the corresponding results of the classical elastica. For an increasing length of the beam, the slenderness increases, the critical loads approach those of Euler's classical elastica.

TABLE 4.3: Critical loads P_{cr}/P_e of a simply supported beam using ABAQUS

n	$\nu = 0.5$			$\nu = 0.3$			$\nu = 0.1$		
	λ/π 11	λ/π 22	λ/π 33	λ/π 11	λ/π 22	λ/π 33	λ/π 11	λ/π 22	λ/π 33
1	0.808	0.936	0.969	0.852	0.953	0.978	0.894	0.969	0.985
2	2.37	3.24	3.58	2.61	3.41	3.69	2.90	3.58	3.79
3	4.10	6.20	7.28	4.64	6.71	7.67	5.30	7.27	8.05

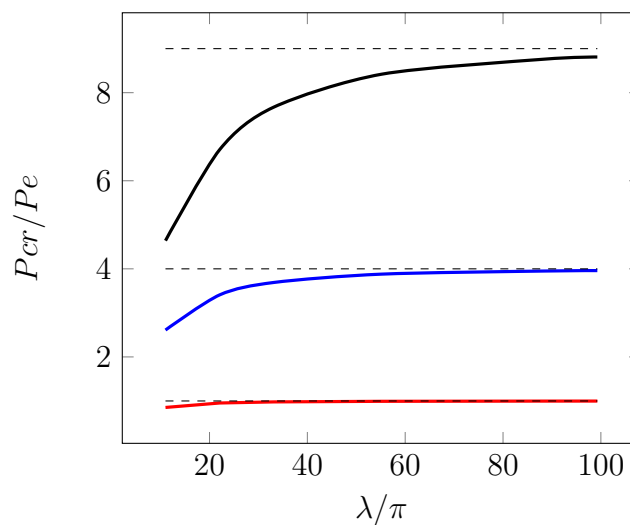


FIGURE 4.1: Critical loads corresponding to the first three buckling modes of a simply supported beam against the slenderness for $\nu = 0.3$ [computed using 3D FEM]

Now, suppose that the shear stiffness exceeds the extensional stiffness, i.e., $\eta > 1$ this correspond with negative value of Poisson's ratio. In Figure 4.2, for smaller values of η which correspond with positive Poisson's ratio, the critical load is smaller than the classical elastica, and it increases for bigger values of η . Consequently, for structure that are very soft in shear, the critical loads are significantly reduced compared with the classical elastica.

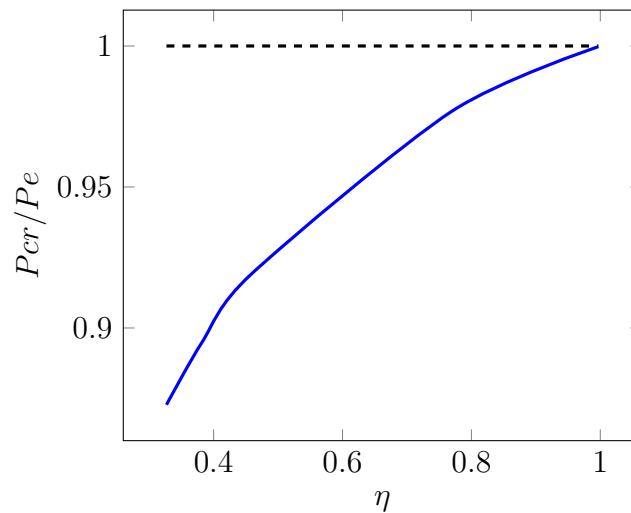


FIGURE 4.2: Critical loads corresponding the first buckling mode of a simply supported beam against the stiffness ratio η ($\lambda/\pi = 11$)[computed using 3D FEM]

4.3 The Cantilever Beam

The same methodology used to determine the critical load for simply supported beam is used for the cantilever beam. At the clamped end, there is no rotation, while the bending moment is zero at the free end.

$$\phi(x = 0) = 0, \quad \frac{\partial \phi}{\partial x} = 0 \quad (4.1)$$

By applying these boundary conditions, the final equation 3.14 presented by Humer to determine the critical load. As in the simply supported beam, the cantilever has the same behavior, if the shear stiffness is lower than the extensional stiffness, the critical loads are below those of Euler's elastica. However, the reverse behavior is observed if the shear stiffness is higher than the extensional stiffness, in which the critical loads are increased.

4.4 Convergence Study

To assess the method of Humer in determining the critical load for simply supported and cantilever beam, a study using ABAQUS software has been conducted, three models were created using the same material used by Humer, the first beam is modeled using 2×2 mesh along the cross-section of the beam, for more accuracy the other models had 4×4 and 8×8 mesh size, respectively, Figure 4.3a shows that the results converge as increasing the mesh size along the cross-section for a simply supported beam. The same analysis have done for the cantilever beam as well in Figure 4.3b.

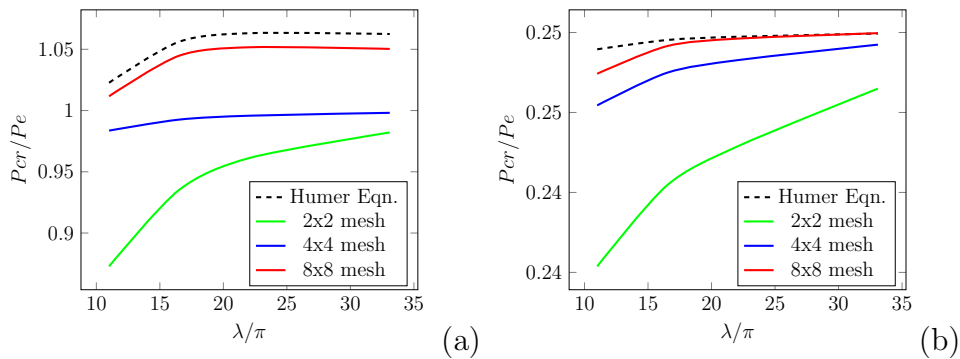


FIGURE 4.3: Critical loads corresponding the first buckling mode against the slenderness ratio (a)S-S Beam (b)C-F Beam [computed using 3D FEM]

4.5 Anisotropic Beams

4.6 Solid rectangular cross-section Beam

Loja and Barbosa [109] developed a finite element model to predict the linear buckling behavior of anisotropic thick and thin beams, using a higher order discrete model (HSDT) in which they assumed a non-linear variation for the displacement field. They developed a two-dimensional composite model which is based on a single layer Lagrangean four node straight beam element and 14 degrees of freedom per node, considering bi-axial bending and stretching. They studied different symmetric and asymmetric layups for various cross-sections. Loja and Barbosa introduced the eigenvalue equation to determine the critical buckling load as

$$Kq = QKq_i + \lambda_i K^G q_i = 0 \quad (4.2)$$

where Q is the system load vector, K and K^G are the system stiffness and geometric matrices, q is the vector of generalized displacements, representing the appropriated Taylor's series terms defined along the x-axis and $z=0$ and $y=0$, and λ_i is the eigenvalue which is a function of the applied loading and the smallest λ_i corresponds to the critical buckling load parameter. By solving these equations with applying the boundary conditions of the system, it can easily obtain the buckling load. Firstly, as a validation study for ABAQUS analysis, a simply-supported rectangular beam has been studied for the buckling behavior of anisotropic beams using ABAQUS software and compared to Euler-Bernoulli (EBT) and Timoshenko beam theory (TBT), the beam cross-section is 1x1m and has the following properties

$$E_1=20.632 \text{ GPa}; E_2=E_3= 4.433 \text{ GPa};$$

$$G_{23}=G_{13}=G_{12}=1.985 \text{ GPa}$$

$$\nu_{13}=\nu_{23}=\nu_{12}=0.318$$

Table 4.4, shows the results obtained by ABAQUS and Euler-Bernoulli theory. It is well known that as the slenderness ratio increases the Euler-Bernoulli almost coincide the elasticity theory results (ELT), the analysis has been conducted for 3 layups with 0° orientation.

The clamped-free anisotropic beam is also considered as a case study in this section.

Table 4.5, shows the critical buckling loads for different slenderness ratios with layups orientation of 0° .

TABLE 4.4: Critical buckling load for simply-supported rectangular composite beam of stacking sequence $[0]_3$

Slenderness Ratio	ELT	EBT	Ratio (EBT/ET)
17	522000	678077	1.3
85	18968	27123.10	1.1
150	3543.8	6780.7	1.1
346	1540	1695.2	1.1

TABLE 4.5: Critical buckling load for cantilever rectangular composite beam of stacking sequence $[0]_3$

Slenderness Ratio	ELT	EBT	Ratio (EBT/ET)
17	140000	169519.4	1.3
85	6123	6780.8	1.1
150	1534	1695.2	1.1
346	383.6	423.8	1.1

4.7 Open cross-section (I-Beam)

The same material properties for the rectangular beam are used here. Table 4.6 shows the buckling load for a simply supported I-beam using different theories, all the cross-sections

studied in this section have 0° layups orientation.

TABLE 4.6: Critical buckling load for simply-supported I-beam cross-section $102 \times 102 \times 6.4 \text{ mm}$

Slenderness Ratio	HSDT (KN)	ELT (KN)	EBT (KN)
70	26.09	25.58	77.10
105	11.60	10.99	34.11
188	–	4.367	10.70
236	–	2.94	6.84
283	–	2.13	4.76
354	–	1.93	3.04

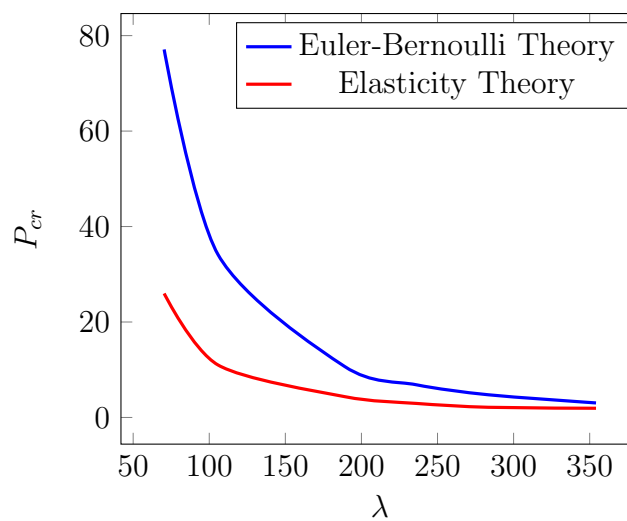


FIGURE 4.4: Critical loads corresponding to the first buckling mode of an anisotropic simply supported I-section beam against the slenderness ratio [computed using 3D FEM]

There is many studies of the buckling of anisotropic beams, Kim et al. [111] in their paper discussed the flexural-torsional buckling loads for spatially coupled stability analysis of thin-walled composite beams, they present the exact element stiffness matrix theory that can be used in analyzing the stability problems of thin-walled composite I-beam made from fiber-reinforced laminates. they studied the coupling effect of a beam subjected to lateral load, some assumptions were introduced to derive the spatially coupled stability analysis of thin-walled composite beam, such as, the strains are assumed to be small, the beam is linearly elastic, and the cross-section is assumed to maintain its shape during

deformation. The equation was obtained to determine the buckling load as follows

$$F_{cr} = \frac{1}{2} \sqrt{\left\{ \frac{1}{R_p^2} \left(JG + \frac{\pi^2 I_\phi}{L^2} \right) + \frac{\pi^2 I_3}{L^2} \right\}^2 - \frac{4}{R_p^2} \left(\frac{\pi^4 I_3 I_\phi}{L^4} + \frac{\pi^4 JG I_3}{L^2} - 1 \right) + \frac{1}{2R_p^2} \left(JG + \frac{\pi^2 I_\phi}{L^2} \right)} \quad (4.3)$$

To demonstrate the accuracy of the stiffness matrix Kim et al. used two finite element methods to validate the stiffness matrix, the Hermitian beam elements and ABAQUS's shell element. In this study, 3D beam modeled using ABAQUS brick elements to assess the stiffness matrix method (SMM), and to compare it with the ABAQUS shell elements results introduced by Kim. Symmetric I-section is adopted for this study with flange width $b=5$ cm and height $h=5$ cm, and thickness $t=0.316$ cm. The material of beams used is glassy-epoxy and its material properties as follows:

$$E_1=53.78 \text{ GPa}, E_2 = E_3=17.93 \text{ GPa},$$

$$G_{12} = G_{13}=8.96 \text{ GPa}, G_{23}=3.45 \text{ GPa},$$

$$\nu_{12} = \nu_{13}=0.25, \nu_{23}=0.34$$

where subscripts '1' and '2' correspond to directions parallel and perpendicular to fibers, respectively. Two boundary conditions configurations are applied at the end supports of the I-beam, clamped-free beam (C-F) and simply supported beam (S-S).

It can be found that the results from SMM are in an excellent agreement with the ABAQUS's solution and Hermitian beam elements, however, it is noticeable that the results obtained by ABAQUS are smaller than the stiffness matrix ones, since the elasticity theory allows for more flexibility. For length $L = 100\text{cm}$ the first eigenvalue was determined for C-F beam using two types of laminate orientation, $[0^\circ]$ and $[90^\circ]$ using 16 laminates, Figure 4.5. The Eigenvalues are obtained for the two orientations as shown in Table 4.7.

The critical buckling load for S-S configuration is also determined using the same orientation that used before, Table 4.8 shows that the results are almost coincide with the results determined by SMM and Hermitian beam elements.

TABLE 4.7: Buckling Loads (N) of C-F beam with doubly symmetric I-section (L=100cm)

Stacking Sequence	SMM	Hermitian Beam Elements	3D ABAQUS Model
$[0]_{16}$	5755.2	5755.2	5718.0
$[0/90]_{4S}$	3857.8	3857.8	3742.3

TABLE 4.8: Buckling Loads (N) of S-S beam with doubly symmetric I-section (L=400cm)

Stacking Sequence	SMM	Hermitian Beam Elements	3D ABAQUS Model
$[0]_{16}$	1438.8	1438.8	1394.4
$[0/90]_{4S}$	964.4	964.4	893.5

More analysis has conducted using the classical Euler buckling formula, for anisotropic material with E_x , E_y , and E_z where E_x , E_y are the modulus of elasticity lie in the plane of the cross-section, and E_z is modulus of elasticity parallel to the longitudinal length of the beam. In Euler Equation, E_z will be used to determine the critical buckling load. A hollow beam is adopted to demonstrate that Results obtained using Euler Equation are plotted with the results obtained from ABAQUS against the slenderness ratio in Figure 4.6.

In the following example, a three-dimensional elasticity model is created and parametric studies were conducted to provide the effects of variation in material characteristics of laminated composite plates on their buckling characteristics. The orthotropic cantilever beam were considered, as mentioned before that the elastic modulus in the z – *direction* is used to determine the buckling load, the angle with respect to x_3 – *direction* is varied

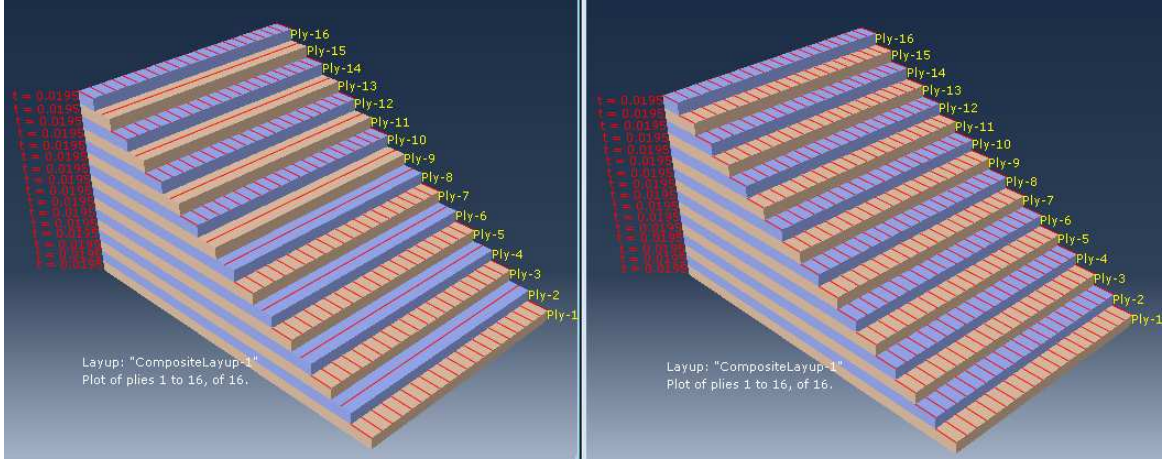


FIGURE 4.5: Laminates orientation for symmetric I-section with total thickness $0.312\text{cm} [(0/90)_{4S},(0)_{16}]$

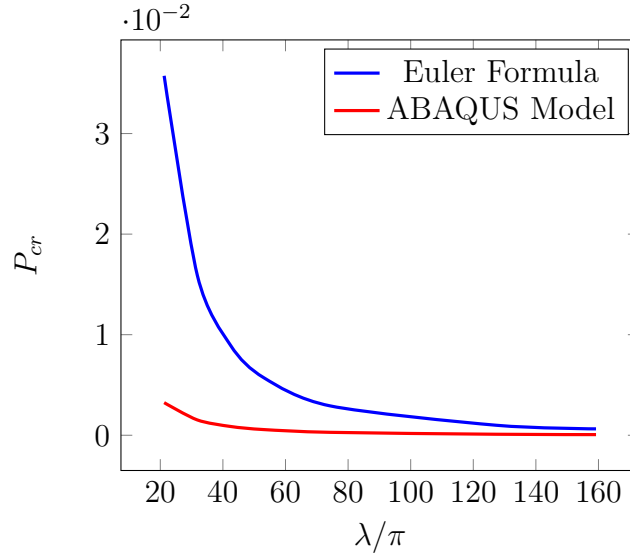


FIGURE 4.6: Critical loads corresponding to the first buckling mode of an anisotropic simply supported beam against the slenderness ratio [computed using 3D FEM]

between 0° and 90° , where the 0° is along the z – *direction* and the 90° is along the cantilever cross-section. Table 4.9 shows the results of the buckling load with the variation in the angle of the elastic modulus along the length direction for different angles between 0° and 90° .

TABLE 4.9: Buckling load of C-F beam with variation in the angle of the laminate

θ	0	10	20	30	40	50	60	70	80	90
Buckling load ($\cdot 10^{-3}$)	4.3	3.7	2.7	1.9	1.5	1.3	1.2	1.1	1.1	1.1

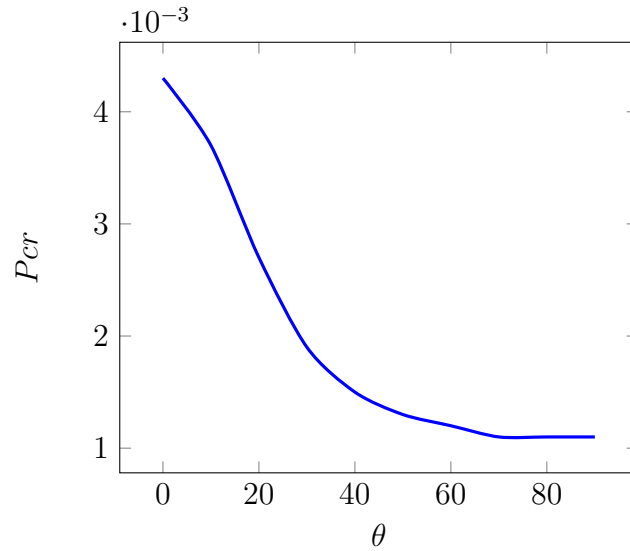


FIGURE 4.7: Buckling loads (KN) of C-F beam corresponding to different ply-angles [computed using 3D FEM]

4.8 Closed cross-Section (Hollow-rectangular Beam)

T.P. Vo, J. Lee [112] studied the flexural-torsional behavior for thin-walled composite beams subjected to axial load. they developed a displacement-based one-dimensional finite element model to predict the critical loads and corresponding buckling modes for a thin-walled symmetric and un-symmetric composite bar. The hollow rectangular cross-section is adopted in this section to compare their results with the ones computed by ABAQUS. The beam cross-section is (2x1)m with length 40m, The beam material properties can be defined as follow

$$E_1=144 \text{ GPa}, E_2=E_3=9.65 \text{ GPa}$$

$$G_{12}=G_{13}=G_{23}=4.14 \text{ GPa}$$

$$\nu_{12}=\nu_{13}=\nu_{23}=0.3$$

The eigenvalue developed by T.P. Vo, J. Lee [112] can be expressed by

$$([K] - \lambda[G])\Delta = 0 \quad (4.4)$$

where $[K]$ and $[G]$ are the element stiffness matrix and the element geometric matrix, respectively. Δ is the eigenvector of nodal displacement corresponding to an eigenvalue, the matrices form can be found in T.P. Vo, J. Lee [112]. Table 4.11 shows the results for the critical buckling load obtained by the 3D elasticity model (ELT) and the one-dimensional finite element model (ODFE). From Table 4.11 it can be seen that the results using the one-dimensional are match the ones by 3D model except for $[45,-45,-45,45]$, that because zero plain stress $E_z = 0$ is considered for the first theory, therefore the model only consider the linearity of the elastic modulus E_x or E_y in which 0° and 90° , and will deviate of the exact solution for diagonal orientations (45°).

Now let consider the buckling behavior corresponding to different lengths and compare

TABLE 4.10: Buckling loads with different stacking sequences and boundary conditions

Boundary Conditions	Stacking Sequence	ODFE	ELT
S-S Beam	[0/0/0/0]	5.196	5.43
	[0/90/90/0]	2.770	3.04
	[45/-45/-45/45]	0.541	1.47
C-F Beam	[0/0/0/0]	1.299	1.36
	[0/90/90/0]	0.694	0.76
	[45/-45/-45/45]	0.135	0.37

it with the Euler-Bernoulli equation for the same hollow section. Table 4.12 shows the buckling loads for the simply-supported and the cantilever hollow beam, and the results are plotted in Figure 4.8.

TABLE 4.11: Buckling loads with different slenderness ratio and boundary conditions

Boundary Conditions	Stacking Sequence	ODFE	ELT
S-S Beam	[0/0/0/0]	5.196	5.43
	[0/90/90/0]	2.770	3.04
	[45/-45/-45/45]	0.541	1.47
C-F Beam	[0/0/0/0]	1.299	1.36
	[0/90/90/0]	0.694	0.76
	[45/-45/-45/45]	0.135	0.37

TABLE 4.12: Buckling loads with different slenderness ratio and boundary conditions

Boundary Conditions	Slenderness Ratio	ELT	EBT
S-S Beam	6.79	0.00153	0.001899669
	13.58	0.000416	0.000474917
	20.37	0.000187	0.00021254
	27.16	0.000106	0.000118729
	40.75	0.0000475	0.0000528
	67.91	0.0000171	0.0000189
C-F Beam	6.79	0.000413	0.000474917
	13.58	0.000106	0.000118729
	20.37	0.0000475	0.000053
	27.16	0.0000267	0.000029
	40.75	0.0000119	0.000013
	67.91	0.00000429	0.0000047

4.9 Auxetic Beams

4.10 Solid rectangular cross-section beam

As it mentioned before, Humer [67] gave an exact solution to predict the critical load. It was found that for value of $\eta < 1$ the buckling load will be less than the classical Euler results, and it matches for $\eta = 1$. For values of $\eta > 1$ which is described as an auxetic material with negative Poisson's ratio. The first studies proposed a micro-structure of the material can be modeled using hexagonal [113, 114] and diamond shape [115]. Lakes [93] studied a compressed foam with the properties $E = 72KPa$ and $\nu = -0.7$, which corresponds to $\eta = 1.163$ for the square section. In this section, the solid rectangular beam

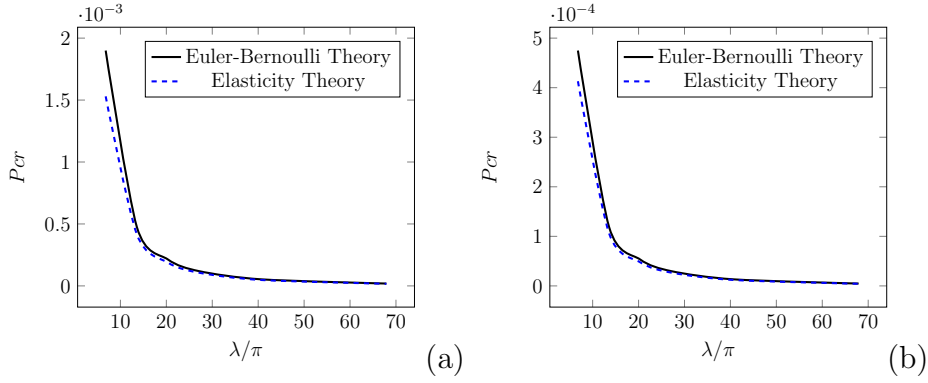


FIGURE 4.8: Critical loads corresponding the first buckling mode of a simply supported anisotropic hollow-beam against the slenderness ratio (a)S-S Beam, (b)C-F Beam [computed using 3D FEM]

is studied for negative Poisson's ratio using Lakes properties [93] and plotted against the ratio λ/π as depicted in Figure 4.9. The theory of Humer [67] concludes that the critical buckling loads are above than the Euler-Bernoulli values for $\eta > 1$, the elasticity theory gives values below the Euler-Bernoulli for $\eta < 1$ as depicted in Figure 4.9. For $\eta > 1$ the elasticity theory gives values above the Euler-Bernoulli.

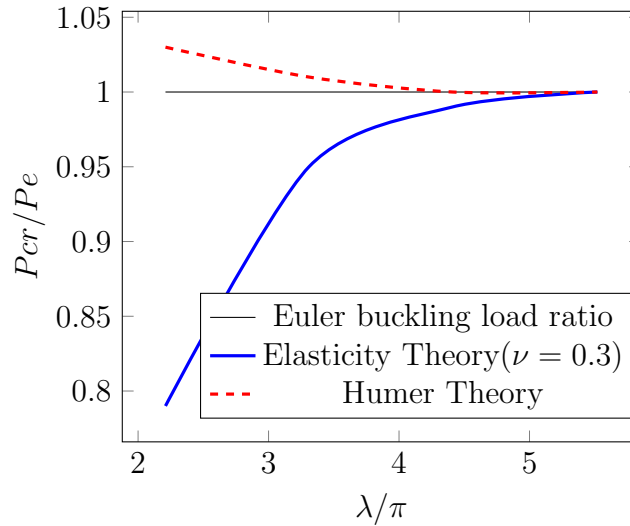


FIGURE 4.9: The first buckling mode of the Simply-supported beam [computed using 3D FEM]

In Figure 4.10 various values of Poisson's ratio were inserted for the case of $\lambda = 5$ which is considered a short beam, it can be seen that the change in behavior changes at much

lower negative value for the elasticity model.

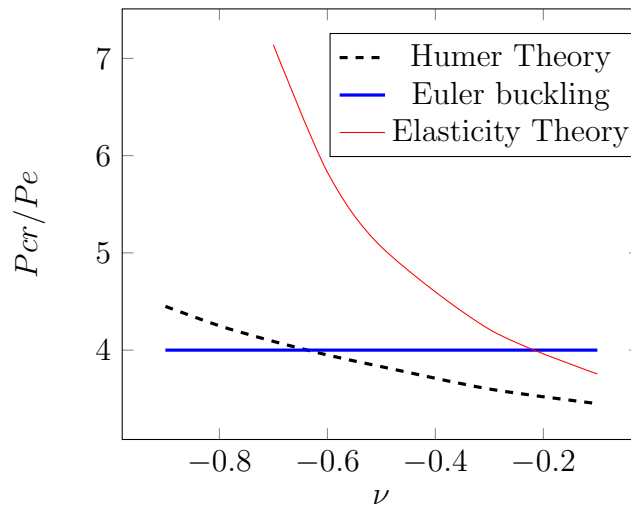


FIGURE 4.10: The second buckling mode of the Simply-supported beam with the properties of Lakes [93] ($\lambda/\pi = 5$) [computed using 3D FEM]

Open Section Beams

The auxetic behavior of open sections has been studied in this section, the I-section beam 102x102x6.4mm is adopted, and the material properties is $E = 72KPa$ and $\nu = -0.3$. The Euler-bernoulli was applied to determine the critical buckling load and compared with the results obtained by the elasticity theory for different beam lengths. In Figure 4.11 the buckling load ratio is plotted against the slenderness ration. The same analysis has conducted to study the cantilever behavior due to buckle, Figure 4.12 shows the buckling load ratio against the slenderness ratio [computed using 3D FEM]

Closed section Beams

The hollow rectangular beam is of interest in this section, the auxeticity behavior for the hollow cross-section is discussed by Lim [112], he discussed the buckling load for

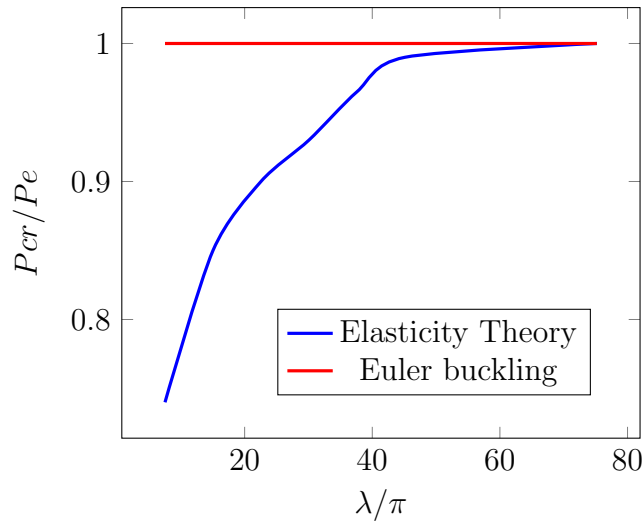


FIGURE 4.11: Critical buckling load for a Simply-supported I-beam ($\nu = -0.3$).

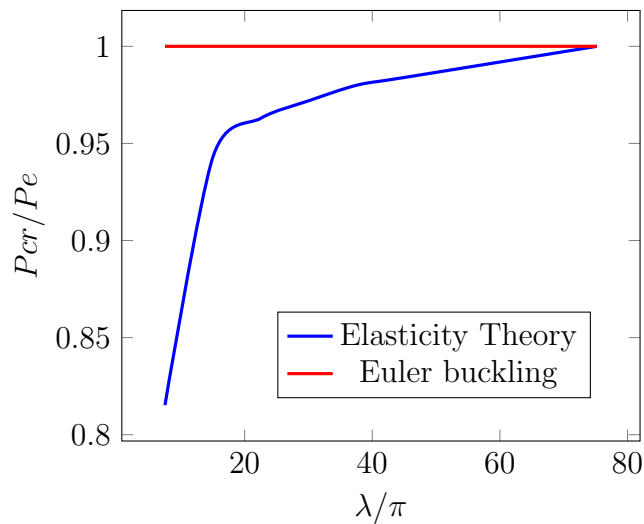


FIGURE 4.12: Critical buckling load for a clamped-free I-beam ($\nu = -0.3$) [computed using 3D FEM]

a shell cylinder with negative Poisson ratio, and he plotted a graph for the buckling load with changing in the ratio between the length to the cylinder radius. The hollow rectangular cross-section 200x100mm with thickness 25mm, $E = 72KPa$, is analyzed using Euler-Bernoulli equation and elasticity based using ABAQUS for $\lambda/\pi = 8$ and $\lambda/\pi = 42$. In Figure 4.13(a-b) which shows the buckling ratio against the Poisson ratio for each slenderness ratio, the figure concludes that as the increasing of the slenderness the intersection between the elasticity theory and the Euler-Bernoulli theory move towards

positive values of Poisson ratio.

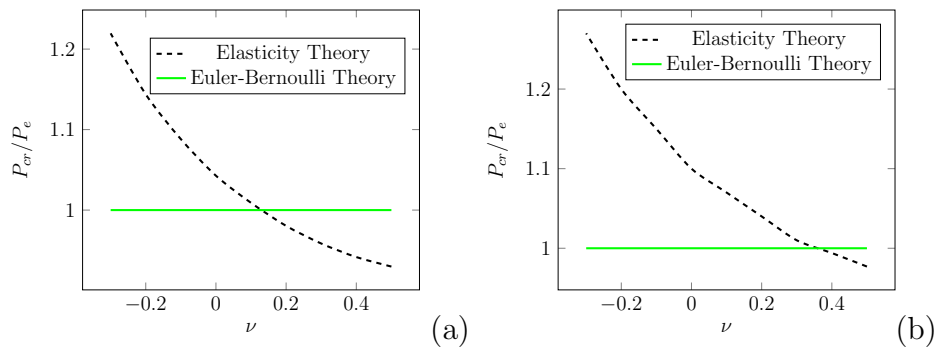


FIGURE 4.13: Critical buckling load of the first mode for a Simply-supported Hollow rectangular beam.(a) $\lambda/\pi = 8$, (b) $\lambda/\pi = 42$ [computed using 3D FEM]

The same analysis has been done for the cantilever of the hollow rectangular beam for the same slenderness ratios, as depicted in Figure 4.14.

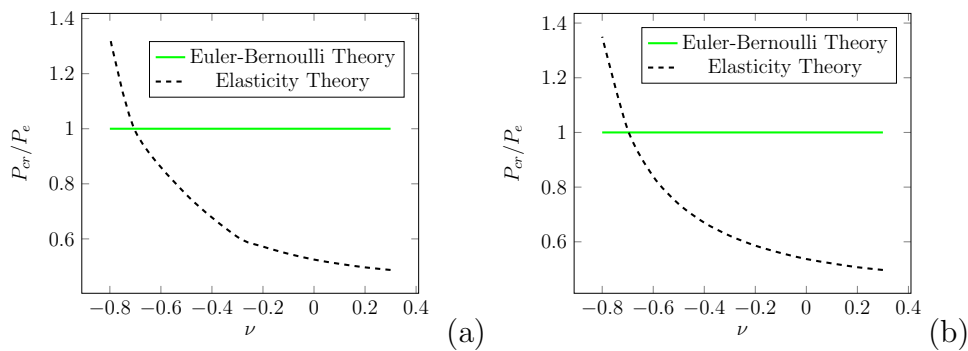


FIGURE 4.14: Critical buckling load of the first mode for a cantilevered Hollow rectangular beam.(a) $\lambda/\pi = 8$, (b) $\lambda/\pi = 42$ [computed using 3D FEM]

4.11 Other Geometries

Lim [101] studied the elastic stability of circular plates made from auxetic materials under various boundary conditions. He determined the critical buckling load factors using Bessel functions for isotropic materials with Poisson's ratios values range between -1 to 0.5 . Results for elastic stability reveal that as the Poissons ratio of the plate becomes more negative, the critical bucking load gradually reduces.

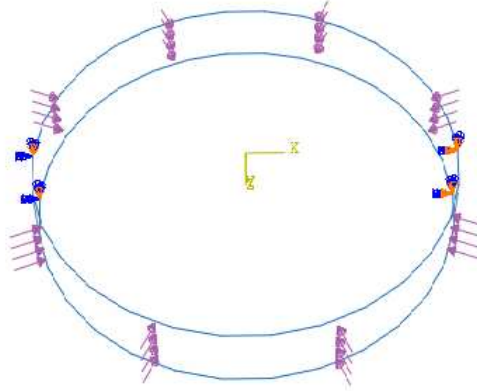


FIGURE 4.15: Cylinder plate with clamped edge

For the cylinder plate shows in Figure 4.15, has the following properties as $E = 2.6$, $h = 0.25$ and $R = 1$, Lim derived the critical buckling load equation as

$$N_{cr} = \bar{N} \frac{D}{R} \quad (4.5)$$

where D is the flexural rigidity of the circular plate and is given by

$$D = \frac{Eh^3}{12(1 - \nu^2)} \quad (4.6)$$

Here h and R is the thickness and radius of the plate, respectively. \bar{N} is the buckling load factors and can be obtained using the empirical model as follows

$$\bar{N} = \bar{n}_0 + \bar{n}_1\nu - \bar{n}_2\nu^2 \quad (4.7)$$

where

$$\begin{Bmatrix} \bar{n}_0 \\ \bar{n}_1 \\ \bar{n}_2 \end{Bmatrix} = \begin{vmatrix} 5.7842 & 12.288 & 9.2057 & -0.5676 & 3.4502 \\ 0.8968 & 3.3373 & 2.9802 & 1.7714 & 2.8683 \\ 0.3356 & 1.1454 & 0.9659 & 0.4226 & 0.5476 \end{vmatrix} \begin{Bmatrix} +(\tan^{-1}(\beta))^4 \\ -(\tan^{-1}(\beta))^3 \\ +(\tan^{-1}(\beta))^2 \\ -(\tan^{-1}(\beta))^1 \\ +(\tan^{-1}(\beta))^0 \end{Bmatrix} \quad (4.8)$$

where β is the rotational stiffness, its value depends on the boundary condition config-

TABLE 4.13: List of computed critical buckling load factor for rotational restraint of S-S and C-F model and Poissons ratio ranges between -1 and 0.5

Region	ν	Rotational restraint, β	
		0	∞
Auxetic	-1.0	0.000	14.6819
	-0.9	0.3934	14.6819
	-0.8	0.7738	14.6819
	-0.7	1.1415	14.6819
	-0.6	1.4969	14.6819
	-0.5	1.8404	14.6819
	-0.4	2.1722	14.6819
	-0.3	2.4927	14.6819
	-0.2	2.8023	14.6819
	-0.1	3.1013	14.6819
Conventional	0.0	3.3900	14.6819
	0.1	3.6687	14.6819
	0.2	3.9379	14.6819
	0.3	4.1978	14.6819
	0.4	4.4487	14.6819
	0.5	4.691	14.6819

urations, for simply supported ($\beta = 0$), while for clamped edge ($\beta = \infty$). In this study, clamped edge will only be considered to be evaluated using 3D ABAQUS model. By determining the critical buckling load using equation 4.5, the results are obtained for each value of Poisson's ratio 4.13 and plotted in Figure 4.16. ABAQUS model is also created

TABLE 4.14: Critical buckling load for a clamped plate corresponding to Lim and elasticity theory

Region	ν	Buckling loads (KN)	
		Lim Theory	Elasticity Theory
Auxetic	-0.9	0.2616	0.1700
	-0.8	0.1381	0.0921
	-0.7	0.0975	0.0657
	-0.6	0.0777	0.0529
	-0.5	0.0663	0.045
	-0.4	0.0592	0.0407
	-0.3	0.0546	0.0377
	-0.2	0.05178	0.0357
	-0.1	0.0502	0.0344
Conventional	0	0.0497	0.0338
	0.1	0.0502	0.0339
	0.2	0.0518	0.0346
	0.3	0.0546	0.036
	0.4	0.0591	0.0395
	0.5	0.0663	0.0500

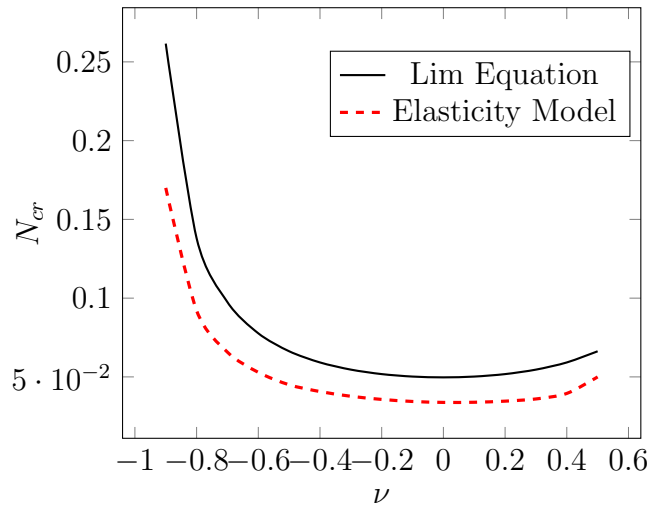


FIGURE 4.16: Critical buckling load plotted against the Poissons ratio [computed using 3D FEM]

as depicted in Figure 4.15 for a clamped cylinder and subjected to uniform load at the edge surface, the ABAQUS results which is based on the elasticity theory are obtained Table 4.14 and plotted with Lim equation in Figure 4.16.

CHAPTER 5

CONCLUSIONS

A continuum finite element study based on 3D elasticity theory using ABAQUS software was conducted to assess the accuracy of beam theories for thin-walled beams of isotropic, anisotropic and auxetic beams. The following highlights were observed

Isotropic Beams

- The elasticity-based loads obtained by ABAQUS were approximately 5 % less than the Humer [67] results for positive Poisson ratio and $\lambda/\pi > 5$.
- Beams with large slenderness ratios coincide with the critical buckling loads determined by Euler-Bernoulli theory, the elasticity to Euler-bernoulli ratio approach its maximum value for $\lambda/\pi < 10$ in case of simply supported rectangular beams.

Anisotropic Beams

- The elasticity based loads are about 20% less than loads obtained by the Euler-Bernoulli theory for $\lambda/\pi < 5$ for simply supported and cantilever beam.
- For open cross-section beams the elasticity theory is about 1% less than the HSDT derived by Loja and Barbosa [109], and for values of $\lambda/\pi = 100$ it matches the values obtained by Euler-Bernoulli theory.
- For closed cross-section beams, the elasticity theory has a good match with the results obtained by Lee [112], and it matches the Euler-Bernoulli for $\lambda/\pi = 700$ which is considered beams with large slenderness ratio.

- The elasticity-based theory results using ABAQUS were within 3 % less than the buckling load predicted by stiffness matrix derived by Kim [111].
- The critical buckling load using the elasticity theory for beams with Young modulus parallel to the longitudinal cross-section is four times larger than its value when the Young modulus is perpendicular to the longitudinal cross-section.

Auxetic Beams

- For values of $\mu > 1$ which correspond to negative Poisson's ratio, the critical buckling load using the elasticity theory is approximately 40 % larger than the buckling load determined by Euler-Bernoulli, and it is significantly reduced for $\mu < 1$.
- The elasticity-based loads obtained by ABAQUS were 20% less than Euler-Bernoulli and Timoshenko beam theories for $\lambda/\pi < 5$ for S-S and C-F beams.
- For the solid cross-section beams, the elasticity theory is about 40 % larger than the Euler-bernoulli buckling load for $-0.9 > \nu > -0.2$ and $\lambda/\pi = 5$ for S-S and C-F beams.
- For open cross-section beams, the elasticity theory results were approximately 20 % less than the Euler-Buckling Load for $\lambda/\pi > 10$ for S-S and C-F beams.
- For S-S closed cross-section beams, as the slenderness ratio increases the intersection between the elasticity and Euler-Bernoulli theory moves towards to the positive values of Poisson ratio.
- For C-F closed cross-section beams for values of λ/π between 8 and 42, the elasticity theory was below the Euler-Bernoulli buckling load for values of $-0.7 > \nu > 0.5$.

- The results obtained by Lim [116] suggest that beam deflection error arising from the use of Euler-Bernoulli beam theory is reduced if the beam material is auxetic, and the error diminishes as the Poisson's ratio approached a value of -1 for the square cross-sectional beams.

BIBLIOGRAPHY

- [1] D. C. N. Silvestre, “First-order generalised beam theory for arbitrary orthotropic materials,” *Thin-Walled Structures*, vol. 40, p. 755789, 2002.
- [2] M. NW., “Introduction to the theory of thin-walled structures,” *Oxford: Oxford University Press*,, 1984.
- [3] E. L. Bernoulli J, “Abhandlungen uber das gleichgewicht und die schwingungen der ebenen elastischen kurven,” *Wilhelm Engelmann 175 Leipzig*, 1910.
- [4] G. J. Timoshenko SP, “Theory of elastic stability.,” *McGraw-Hill*, 1961.
- [5] V. SA, “Ustoiczivost deformirujemych system.,” *Science, Moscow*, 1967.
- [6] T. Kubiak, *Static and Dynamic Buckling of Thin-Walled Plate Structures*, vol. 190. Springer, 2013.
- [7] H. G. Davids AJ, “Compression tests of long welded i-section columns.,” *J Struct Eng*, vol. 10, pp. 2281–2297, 1986.
- [8] G.-S. TR, “The local buckling of box girders under bending stresses.,” *Int J Mech Sci*, vol. 11, pp. 603–612, 1969.
- [9] P. T. Mulligan GP, “Locally buckled thin-walled columns.,” *J Struct Eng*, vol. 110(11), pp. 2635–2654, 1961.
- [10] P. M. Grimaldi A, “Post-buckling behaviour of thin-walled open cross-section compression members.,” *J Struct Mech*, vol. 7(2), pp. 143–159, 1979.

- [11] v Koiter WT, “Elastic stability and post-buckling behaviour.,” *Proceedings of the Symposium on Non-linear Problems, Univ. of Wisconsin Press, Wisconsin*, pp. 257–275, 1963.
- [12] K. M, “Statecznosc, stany zakrytyczne i nosnosc graniczna cienkosciennych dzwigarow o scianach plaskich. series of monographs,” *Technical University of Lodz Press.*, 1995.
- [13] P. M. Koiter WT, “A general theory for the interaction between local and overall buckling of stiffened panels.,” *WTHD, Report No. 556, Delft University*, 1976.
- [14] v. d. N. A. Koiter WT, “Interaction between local and overall buckling of stiffened compression panels.,” *part I :5156 and part II :6686. In: Rhodes J, Walker AG (eds) Thin-Walled Structures. Granada, St.Albans, London*, 1980.
- [15] H. J. Byskov E, “Mode interaction in axially stiffened cylindrical shells.,” *AIAA J* 15, vol. 15(7), pp. 941–948, 1977.
- [16] S. S. Ali MA, “A versatile model for interactive buckling of columns and beam-columns.,” *Int J Solids Struct*, vol. 24(5), pp. 481–486, 1988.
- [17] S. S. Benito R, “Mode interaction in thin-walled structural members.,” *J Struct Mech*, vol. 12(4), pp. 517–542, 1985.
- [18] B. E, “Elastic buckling problem with innitely many local modes.,” *Mech Struct Mach*, vol. 15(4), pp. 413–435, 1988.
- [19] P. M. Koiter WT, “An alternative approach to the interaction between local and overall buckling in stiffened panels.,” *Buckling of structures Proceedings of IUTAM Symposium, Cambridge*, pp. 133–148, 1974.

- [20] K. Z, “Influence of modification of boundary conditions on load carrying capacity in thin-walled columns in the second order approximation.,” *Int J Solid Struct*, vol. 30(19), pp. 2597–2609, 1993.
- [21] M. AI, “Sviazannaja poteria ustoicivosti srzatoi podkrepljennoi paneli.,” *Mekh Tverd Tela.*, vol. 23(5), pp. 152–159, 1988.
- [22] G. P. Moellmann M, “Interactive buckling in thin-walled beams, part i: Theory, part ii: Applications.,” *Int J Solid Struct*, vol. 25(7), pp. 715–728, 1989.
- [23] S. E, “The critical shear load of rectangular plate.,” *NACA TM*, vol. 705, 1933.
- [24] S. RCT, “The buckling of at plywood plate in compression.,” *Australian Council for Aeonautics Rep. 12*, 1944.
- [25] S. Y. Reissner E, “Bending and stretching of certain types of heterogeneous aelotropic elastic plates,” *Trans ASME J Appl. Mech.*, vol. 9, pp. 402–408, 1961.
- [26] L. S, “Anisotropnyje plastinki.,” *Moscow-Leningrad*, 1947.
- [27] A. SA, “Theory of anisotropic plates,” *Technomic*, 1970.
- [28] W. J. Ashton JE, “Theory of laminated plates,” *Technomic*, 1970.
- [29] C. T. Vinson JR, “Composite materials and their use in structures,” *Applied Science Publisher Ltd*, 1975.
- [30] M. H, “Buckling of at plywood plates in compression, shear or combined compression and shear.,” *Forest Products Laboratory Rep. 1316*, 1942.
- [31] M. R. Fraser HR Jr, “Bifurcation type of buckling of generally orthotropic clamped plates.,” *AIAA J.*, vol. 8(4), pp. 707–771, 1970.

- [32] M. JM, “An experimental study of the postbuckling of anisotropic plates.,” *MSc thesis, Case Western Reserve University*, 1968.
- [33] N. AK, “Stability of multilayered composite plates.,” *Fibre Sci Technol*, vol. 8, pp. 81–89, 1975.
- [34] R. B. Chandra R, “Postbuckling analysis for rectangular orthotropic plates.,” *Int J of Mech Sci*, vol. 16, pp. 81–97, 1973.
- [35] C. C. Prahakara MK, “Postbuckling behaviour of rectangular orthotropic plates.,” *J Mech Eng Sci*, vol. 17, pp. 25–33, 1973.
- [36] M. C, “The elastic buckling of orthotropic rectangular plates.,” *Civ Eng Trans*, vol. 13(1), pp. 63–65, 1971.
- [37] O. G. Brunelle EJ, “Generic buckling curves for specially orthotropic rectangular plates.,” *AIAA J*, vol. 21(8), pp. 1150–1156, 1983.
- [38] Y. Cheung, *Finite strip method in structural analysis*. Pergamon Press, 1976.
- [39] A. Z. Dawe DJ, Lam SSE, “Finite strip post-local-buckling analysis of composite prismatic plate structures.,” *Comput Struct*, vol. 48(6), pp. 1011–1023, 1993.
- [40] S. S. Kasagi A, “Postbuckling analysis of layered composites using p-version nite strips.,” *Int J Numer Meth Eng*, vol. 33, pp. 2091–2107, 1992.
- [41] M. Mahendran and N. W. Murray, “Elastic buckling analysis of ideal thin-walled structures under combined loading using a finite strip method,” *Elsevier*, pp. 329–360, 1986.

- [42] A. J. Davids and G. J. Hancock, “Compression tests of long welded i-section columns,” *J. Struct. Eng.*, vol. 112, pp. 2281–2297, 1986.
- [43] Eccher and Rasmussen, “Isoparametric spline finite strip method for in-plane stress analysis,” *The University of Sydney*, 2005.
- [44] W.-L. T. Hsuan-Teh Hu, “Buckling analysis of skew composite laminate plates.,” *International Conference On Composite Materials, Gold Coast, Queensland Australia*, 1997.
- [45] R. J. Bao G, Jiang W, “Analytic and nite element solutions for bending and buckling of orthotropic rectangular plates.,” *Int J Solid Struct*, vol. 34(14), pp. 1797–1822, 1997.
- [46] T. J. Barbero E, “Euler buckling of thin-walled composite columns,” *Thin-Walled Struct*, vol. 17, pp. 237–258, 1993.
- [47] R. K. Gupta RK, “Instability of laminated composite thin-walled open-section beams.,” *Compos Material.*, vol. 4, pp. 299–313, 1985.
- [48] K. V. Awrejcewicz J, “Nonclassical thermoelastic problems in nonlinear dynamics of shells.,” *Springer-Verlag, Berlin*, 2003.
- [49] M. L. Awrejcewicz J, Andrianov IV, “Asymptotical mechanics of thin-walled structures. a handbook.,” *Springer-Verlag, Berlin*, 2004.
- [50] V. A. Awrejcewicz J, Krysko VA, “Nonlinear dynamics of continuos elastic systems.,” *Springer-Verlag, Berlin*, 2004.
- [51] S. C, “Stability and initial post-buckling behaviour of frame system with vertical bracings.,” *Thin-Walled Struct*, vol. 49(5), pp. 669–673, 2011.

- [52] S. C. W. W. Chroscielowski J, Lubowiecka I, “On some aspects of torsional buckling of thin-walled i-beam columns.,” *Comput Struct*, vol. 84(29-30), pp. 1946–1957, 2006.
- [53] U. S. Tomski L, Szmidla J, “The local and global instability and vibration of systems subjected to non-conservative loading.,” *Thin-Walled Struct*, vol. 45(10-11), pp. 945–949, 2007.
- [54] U. S. Tomski L, “Free vibrations and the stability of a geometrically non-linear column loaded by a follower force directed towards the positive pole.,” *Int J Solids Struct*, vol. 45(1), pp. 87–112, 2008.
- [55] P.-B. I. Tomski L, “Global buckling and the interaction of initial imperfections of columns subjected to conservative loading.,” *Thin-Walled Struct*, vol. 49(5), pp. 87–112, 2008.
- [56] I. P. r.-B. L. Tomski, “Global buckling and the interaction of initial imperfections of columns subjected to conservative loading,” *Thin-Walled Structures*, vol. 49(2011), pp. 596–603, 2010.
- [57] K. Z. Teter A, “Buckling of thin-walled composite structures with intermediate stiffeners.,” *Compos Struct*, vol. 69(4), pp. 421–428, 2005.
- [58] K. Z. Teter A, “Interactive buckling and load carrying capacity of thin-walled beam-columns with intermediate stiffeners.,” *Thin-Walled Struct*, vol. 42, pp. 211–254, 2004.
- [59] G. A. Rzeszut K, “Modeling of initial geometrical imperfections in stability analysis of thin-walled structures.,” *J Theor Appl Mech*, vol. 47(3), pp. 667–684, 2009.

- [60] G. A. Rzeszut K, “Thin-walled structures with slotted connections stability problems.,” *Thin-Walled Struct*, vol. 49(5), pp. 674–681, 2011.
- [61] M. K. Magnucka-Blandzi E, “Buckling and optimal design of cold-formed thin-walled beams.review of selected problems.,” *Thin-Walled Struct*, vol. 49(5), pp. 554–561, 2011.
- [62] P. P. Magnucki K, “Theoretical shape optimization of cold-formed thin-walled channel beams with drop anges in pure bending.,” *J Constr Steel Res*, vol. 56(8-9), pp. 1731–1737, 2009.
- [63] K. J. Magnucki K, Paczos P, “Elastic buckling of cold-formed thin-walled channel beams with drop flanges,” *J Struct Eng*, vol. 136(7), pp. 886–896, 2010.
- [64] Z. J. Paczos P, “Stability of orthotropic elastic-plastic open conical shells.,” *Thin-Walled Struct*, vol. 46(5), pp. 530–540, 2008.
- [65] Z. J. Jaskula L, “Large displacement stability analysis of elasticplastic unsymmetrical sandwich cylindrical shells.,” *Thin-Walled Struct*, vol. 49(5), pp. 611–617, 2011.
- [66] J. Zielnica, “Buckling and stability of elastic-plastic sandwich conical shells.,” *Steel Compos Struct*, vol. 13(2), pp. 157–169, 2012.
- [67] A. Humer, “Exact solutions for the buckling and postbuckling of shear-deformable beams.,” *Acta Mech*, vol. 224, pp. 1493–1525, 2013.
- [68] K.-M. K. Kolakowski Z, “Static, dynamic and stability of structures, vol. 2: Statics, dynamics and stability of structural elements and systems.,” *Technical University of Lodz Press*, 2012.

- [69] K. M. Kolakowski Z, “Modal coupled instabilities of thin-walled composite plate and shell structures.,” *Compos Struct*, vol. 76, pp. 303–313, 2006.
- [70] K.-M. K. Kolakowski Z, “Interactive buckling regarding the axial extension mode of a thin-walled channel under unifor compression in the rst nonlinear approximation.,” *Int J Solids Struct*, vol. 48(1), pp. 119–125, 2011.
- [71] M. R. S. J. Krolak M, Kowal-Michalska K, “Experimental tests of stability and load carrying capacity of compressed thin-walled multi-cell columns of triangular cross-section.,” *Thin-Walled Struct*, vol. 45(10-11), pp. 883–887, 2007.
- [72] M. R. S. J. Krolak M, Kowal-Michalska K, “Stability and load carrying capacity of multi-cell thin-walled columns of rectangular cross-sections.,” *J Theor Appl Mech*, vol. 47(1), pp. 435–456, 2009.
- [73] M. R. Krolak M, “Critical and postcritical behavior of thin walled multicell column of open prole.,” *Mech Mech Eng*, vol. 14(2), pp. 281–290, 2010.
- [74] J. K. Loughlan J, Yidris N, “The failure of thin-walled lipped channel compression members due to coupled local-distortional interactions and material yielding.,” *Thin-Walled Struct*, vol. 61, pp. 14–21, 2012.
- [75] C. P. Loughlan J, Yidris N, “The effects of local buckling and material yielding on the axial stiffness and failure of uniformly compressed i-section and box-section struts.,” *Thin-Walled Struct*, vol. 49(2), pp. 264–279, 2011.
- [76] G. S. Ovesy HR, Loughlan J, “An investigation on the post-local-buckling analysis of i-section struts using nite strip method.,” *Adv Steel Constr*, vol. 6(1), pp. 662–677, 2010.

- [77] K. M. Macdonald M, Rhodes J, “Stainless steel stub columns subject to combined bending and axial loading.,” *Thin-Walled Struct*, vol. 45(10-11), pp. 893–897, 2007.
- [78] R. J. Macdonald M, Heiyantuduwa MA, “Recent developments in the design of cold-formed steel members and structures.,” *Thin-Walled Struct*, vol. 46(7-9), pp. 1047–1053, 2008.
- [79] R. J, “Some recent research on thin-walled members at the university of strathclyde.,” *Thin-Walled Struct*, vol. 45(10-11), pp. 821–826, 2007.
- [80] C. D. Goncalves R, Dinis PB, “General beam theory formulation to analyse the first-order and buckling behaviour of thin-walled members with arbitrary cross-sections.,” *Thin-Walled Struct*, vol. 47(5), pp. 583–600, 2009.
- [81] S. Schafer BW, Adany, “Buckling analysis of cold-formed steel members using cufsm: conventional and constrained finite strip methods.,” *In: Proc. 18th International Specialty Conference on Cold-Formed Steel Structures, Orlando, Florida*, 2006.
- [82] A. Love, “A treatise on the mathematical theory of elasticity.,” 1944.
- [83] I. H. S. R. K.E. Evans, M.A. Nkansah, “Molecular network design,” *Nature* 353, 1991.
- [84] D. G. R.H. Baughman, “Crystalline networks with unusual predicted mechanical and thermal properties,” *Nature* 365, pp. 735–737, 1993.
- [85] K. E. J.N. Grima, “Self-expanding molecular networks,” *Chem. Commun.* 16, pp. 1531–1532, 2000.

- [86] K. E. J.N. Grima, J.J. Williams, “Networked calixarene polymer with unusual mechanical properties,” *Chem. Commun.*, pp. 4065–4067, 2005.
- [87] A. G. C.B. He, P.W. Liu, “Toward negative poisson ratio polymer through molecular design,” *Macromolecules* 31, pp. 3145–3147, 1998.
- [88] A. Z. S. S. R.H. Baughman, J.M. Shacklette, “Negative poisson’s ratios as a common feature of cubic metals,” *Nature* 392, pp. 362–365, 1998.
- [89] J. P. A. Yeganeh-Haeri, D.J. Weidner, “Elasticity of acristobalite: A silicon dioxide with a negative poisson’s ratio,” *Science* 257, pp. 650–652, 1992.
- [90] A. A. K. E. J.N. Grima, R. Jackson, “Do zeolites have negative poisson’s ratio ?,” *Adv. Mater.* 12, pp. 1912–1918, 2000.
- [91] K. E. K.L. Alderson, “Strain-dependent behaviour of microporous polyethylene with a negative poisson’s ratio,” *J. Mater Sci.* 28, pp. 4092–4098, 1993.
- [92] K. E. A.P. Pickles, K.L. Alderson, “The effects of powder morphology on the processing of auxetic polypropylene,” *Polym. Eng. Sci.* 36, pp. 636–642, 1996.
- [93] R. Lakes, “Foam structures with a negative poisson’s ratio,” *Science* 235, pp. 1038–1040, 1987.
- [94] R. S. Lakes, “No contractile obligations,” *Nature*, 358, pp. 713–714, 1992.
- [95] R. Lakes, “Advances in negative poissons ratio materials,” *Advanced Materials*, pp. 293–296, 1993.
- [96] H. O. et al., “Buckling, postbuckling and imperfection-sensitivity: Old questions and some new answers,” *Comput. Mech.*, vol. 37, pp. 498–506, 2006.

- [97] P. K. B. M. T. S. Artur A. Poniak, Henryk Kamiski and K. W. Wojciechowski, “Anomalous deformation of constrained auxetic square,” *Rev. Adv. Mater. Sci.*, vol. 23, pp. 169–174, 2010.
- [98] J. G. et al., “Negative poissons ratios in cellular foam materials,” *Materials Science and Engineering*, pp. 214–218, 2006.
- [99] M. K. W. et al., “Effects of orthotropy and variation of poissons ratio on the behaviour of tubes in pure exure,” *Journal of the Mechanics and Physics of Solids*, vol. 55, pp. 1086–1102, 2007.
- [100] N. Karnesis and G. Burriesci, “Uniaxial and buckling mechanical response of auxetic cellular tubes,” *Smart Mater. Struct.*, vol. 22, p. 9, 2013.
- [101] T.-C. Lim, “Buckling and vibration of circular auxetic plates,” *Engineering Materials and Technology*, vol. 136, 2014.
- [102] T. W. V. Salit, “On the feasibility of introducing auxetic behavior into thin-walled structures,” *Acta Materialia*, vol. 57, pp. 125–135, 2009.
- [103] S. et al., “Negative poissons ratio in hollow sphere materials,” *International Journal of Solids and Structures*, vol. 54, pp. 192–214, 2015.
- [104] R. Brighenti, “Smart behaviour of layered plates through the use of auxetic materials,” *Thin-Walled Structures*, vol. 84, pp. 432–442, 2014.
- [105] A. A.-A. et al., “Using abaqus with 3d imaging techniques for material characterization,” *University of Exeter, UK*, p. 12, 2007.
- [106] P. R. Heyliger, “Continuum-based stability of anisotropic and auxetic beams,” *Mechanics Research Communications*, pp. 1–14, 2015.

- [107] M. Z. Kabir and A. N. Sherbourne, “Local buckling of thin-walled fibre composite beams under transverse loading,” *Can. J. Civ. Eng.*, vol. 26, pp. 107–118, 1999.
- [108] B. T. Visscher WM, Migliori A and R. RA, “On normal modes of free vibration of inhomogeneous and anisotropic elastic objects.,” *Journal of the Acoustical Society of America*, vol. 90, pp. 2154–2162, 1991.
- [109] C. M. M. S. M. A. Ramos Loja, J. Infante Barbosa, “Buckling behaviour of laminated beam structures using a higher-order discrete model,” *Composite structures*, vol. 38, pp. 119–131, 1997.
- [110] E. B. . J. Tomblin, “Euler buckling of thin-walled composite columns,” *Thin- Walled Structures*, vol. 17, pp. 237–258, 1993.
- [111] N.-I. K. et al., “Flexural-torsional buckling loads for spatially coupled stability analysis of thin-walled composite columns,” *Advances in Engineering Software*, vol. 39, pp. 949–961, 2008.
- [112] J. L. Thuc Phuong Vo, “Flexuraltorsional buckling of thin-walled composite box beams,” *Thin-Walled Structures*, vol. 45, pp. 790–798, 2007.
- [113] M. A. L.J. Gibson, “Cellular solids: Structure and properties,” *Pergamon, Oxford*, 1988.
- [114] K. E. I.G. Masters, “Models for the elastic deformation of honeycombs,” *Compos. Struct*, vol. 35, pp. 403–422, 1996.
- [115] K. E. C.W. Smith, J.N. Grima, “Novel honeycombs with auxetic behaviour,” *Acta Mater*, vol. 48, pp. 4349–4356, 2000.

- [116] T. cheng Lim, “Shear deformation in beams with negative poisson’s ratio,” *Materials: design and application*, pp. 427–440, 2014.